İstatistik, Journal of the Turkish Statistical Association
1999, Vol.2, No 3, pp. 145-151

A CHARACTERIZATION OF UNIFORM DISTRIBUTION

M. Ahsanullah.
Rider University, Department of Management Sciences, Lawrenceville, NJ 08648-3099, USA

I. Bairamov
Ankara University, Faculty of Science, Department of Statistics
06100, Tandogan, Ankara, Turkey

Abstract

Let $X_1, X_2, ..., X_n$ be a random sample from a population with probability density function (p.d.f.) $f(x)$, $(x > 0)$, and let $Y_{(1)} = \sum_{i=1}^{n} \frac{X_i}{X_{(n)}}$, where $X_{(n)} = \max_{1 \le i \le n} X_i$. A necessary and sufficient condition based on the statistic $Y_{(1)}$ that an absolutely continuous (with respect to Lebesque measure) p.d.f. $f(x)$, $x > 0$, will be rectangular, is given.

Key Words: Characterization, uniform distribution, Mellin transform

1. Introduction

Stapleton (1963) gave a characterization of the uniform distribution on a compact topological group. His results are as follows: Let $X_1, X_2, ..., X_n$ be n independent random variables taking values in a compact, separable, connected commutative group Γ such that X_j takes for no j all its values in a fixed coset of a proper compact subgroup of Γ. Let $A = (a_{ij})$ be an $n \times n$ matrix of integers such that for each i at least two a_{ij}'s are different from zero and let $\det A = \pm 1$. Suppose that the distribution of X_i $(i = 1, 2, ..., n)$ has an absolutely continuous component with respect to Haar measure on Γ. Let

$$Z_i = \sum_{j=1}^{n} a_{ij} X_j \qquad (i = 1, 2, ..., n); \tag{1.1}$$

if $Z_1, Z_2, ..., Z_n$ are independent then each X_j is uniformly distributed in Γ. Conversely, if $X_1, X_2, ..., X_n$ are independent uniformly distributed random variables with

values in a connected group Γ and if (a_{ij}) is a matrix of integers, then $Z_1, Z_2, ..., Z_n$ defined by (1.1) are independently and uniformly distributed if, and only if, (a_{ij}) is non-singular.

In the present paper we consider the characterization problem based on the statistics

$$\sum_{i=1}^{n} \frac{X_i}{\max(X_1, X_2, ..., X_n)}.$$

2. Main Result

Theorem 1. Let X be a positive random variable having a non-decreasing absolutely continuous probability distribution function F. Then X has probability density function

$$f(x) = \begin{cases} 1/a, & 0 < x \leq a \\ 0, & otherwise \end{cases}, \tag{2.1}$$

if and only if

$$Y_{(1)} \equiv \sum_{i=1}^{n} \frac{X_i}{\max(X_1, X_2, ..., X_n)} \stackrel{d}{=} 1 + \sum_{i=1}^{n-1} U_i \tag{2.2}$$

for some two consecutive values of $n = m$ and $m+1$, where U_i $(i = 1, 2, ..., n-1)$ are independent and uniformly distributed over $(0, 1]$ r.v.'s and $m(> 1)$ is some integer. In (2.1) a is an arbitrary positive number.

Proof. The necessity of condition (2.2) is trivially established by considering the characteristic function of $Y_{(1)}$ (see Darling (1952)) given by

$$\Phi_n(t) = E\left(e^{itY_{(1)}}\right) = ne^{it} \int_0^{\infty} \left[\beta \int_0^1 e^{it\alpha} f(\alpha\beta) d\alpha\right]^{n-1} f(\beta) d\beta. \tag{2.3}$$

Substituting for $f(x)$ as given in (2.1) , we obtain

$$\Phi_n(t) = e^{it} \left(\frac{e^{it} - 1}{it}\right)^{n-1} \tag{2.4}$$

But the characteristic function of $1 + \sum_{i=1}^{n-1} U_i$ is $e^{it} \left(\frac{e^{it}-1}{it}\right)^{n-1}$.

To prove the sufficiency we must prove that the integrofunctional equation

$$n \int_0^{\infty} \left[\beta \int_0^1 e^{it\alpha} f(\alpha\beta) d\alpha\right]^{n-1} f(\beta) d\beta = \left(\frac{e^{it} - 1}{it}\right)^{n-1}. \tag{2.5}$$

has the unique solution (2.1) (except for the arbitrariness of the positive constant a) for some two consecutive values of $n = m$ and $m + 1$ and all real t.

Let us write the left hand side of (2.5) as a multiple integral

$$n \int_0^\infty d\beta f(\beta)\beta^{n-1} \int_0^1 d\alpha_1 ... \int_0^1 d\alpha_{n-1} e^{it(\alpha_1+...+\alpha_{n-1})} f(\alpha_1\beta)...f(\alpha_{r.-1}\beta)$$

Considered as a Lebesque integral , the interchange of β and $\alpha-$integrals is justified since $f(x)$ is a non-negative function for $0 < x < \infty$. Hence we can write this integral as

$$n \int_0^1 d\alpha_1 ... \int_0^1 d\alpha_{n-1} e^{it(\alpha_1+...+\alpha_{n-1})} \int_0^\infty d\beta\beta^{n-1} f(\beta)f(\alpha_1\beta)...f(\alpha_{n-1}\beta). \tag{2.6}$$

The right hand side of (2.5) is obviously equal to

$$\int_0^1 d\alpha_1 ... \int_0^1 d\alpha_{n-1} e^{it(\alpha_1+...+\alpha_{n-1})}. \tag{2.7}$$

Hence the functional equation (2.5) reduces to

$$\int_0^1 d\alpha_1 ... \int_0^1 d\alpha_{n-1} e^{it(\alpha_1+...+\alpha_{n-1})} G(\alpha_1, \alpha_2, ..., \alpha_{n-1}) = 0, \tag{2.8}$$

where

$$G(\alpha_1, \alpha_2, ..., \alpha_{n-1}) \equiv \int_0^\infty d\beta\beta^{n-1} f(\beta)f(\alpha_1\beta)...f(\alpha_{n-1}\beta) - \frac{1}{n}. \tag{2.9}$$

We may assume that $G(\alpha_1, \alpha_2, ..., \alpha_{n-1})$ satisfies a Dirichlet condition (see Sneddon (1951)) in each of the $\alpha-$variables in the $n-1$ dimensional box $0 < \alpha_i \leq 1$ $(i = 1, 2, ..., n-1)$. Let us define a function $H(\alpha_1, \alpha_2, ..., \alpha_{n-1})$ on $-\infty < \alpha_i < \infty$, $(i = 1, 2, ..., n-1)$ such that

$$H(\alpha_1, \alpha_2, ..., \alpha_{n-1}) = \begin{cases} 0 & , \quad -\infty < \alpha_i < 0 \\ G(\alpha_1, \alpha_2, ..., \alpha_{n-1}) & , \quad 0 < \alpha_i \leq 1, (i = 1, 2, ..., n-1) \\ 0 & , \quad 1 < \alpha_i < \infty \end{cases} \tag{2.10}$$

Then $H(\alpha_1, \alpha_2, ..., \alpha_{n-1})$ certainly satisfies a Dirichlet condition in each α_i on the whole space. We then have an 'enlarged' equation

$$\int_{-\infty}^\infty d\alpha_1 ... \int_{-\infty}^\infty d\alpha_{n-1} e^{it(\alpha_1+...+\alpha_{n-1})} H(\alpha_1, \alpha_2, ..., \alpha_{n-1}) = 0 \tag{2.11}$$

By the uniqueness theorem on Fourier transforms, the only solution of (2.11) is the trivial solution

$$H(\alpha_1, \alpha_2, ..., \alpha_{n-1}) = 0 \text{ for } -\infty < \alpha_i < \infty, \ (i = 1, 2, ..., n-1),$$

which implies

$$G(\alpha_1, \alpha_2, ..., \alpha_{n-1}) = 0 \text{ for } 0 < \alpha_i \leq 1, \ (i = 1, 2, ..., n-1) \tag{2.12}$$

almost everywhere.

Hence we are lead to the functional equation

$$\int_0^\infty d\beta \beta^{n-1} f(\beta) f(\alpha_1 \beta) ... f(\alpha_{n-1}\beta) = \frac{1}{n}, \quad n = m, \ m+1, \tag{2.13}$$

where all α_i's are arbitrary except for the restriction $0 < \alpha_i \leq 1$, $(i = 1, 2, ..., n-1)$. In particular, if we set $\alpha_1 = \alpha_2 = ... = \alpha_{n-1} = 1$, then we get

$$\int_0^\infty d\beta \beta^{n-1} f^n(\beta) = \frac{1}{n} \tag{2.14}$$

for $n = m$ and $m+1$.

Convergence of the integral in (2.14) requires that

$$\beta f(\beta) \to 0 \text{ as } \beta \to 0^+ \tag{2.15}$$

and

$$\beta f(\beta) \to 0 \text{ as } \beta \to \infty. \tag{2.16}$$

Expect for the exponent n in $f^n(\beta)$ in equation (2.14) we have a situation similar to the Mellin transform and it is well-known that the inverse Mellin transform of $1/n$ is (see Erdelyi (1954)) $g(\beta)$, given by

$$g(\beta) = \begin{cases} 1 & , \ 0 < \beta < 1, \\ 0 & , \ \beta > 1. \end{cases} \tag{2.17}$$

In fact, this is also a solution of (2.14) as can be easily verified. A slight generalization of (2.17) satisfying (2.15) and (2.16) is given by

$$\delta_a(\beta) = \begin{cases} 1/a & , \ 0 < \beta \leq a, \\ 0 & , \ \beta > a. \end{cases} \tag{2.18}$$

This also satisfies equation (2.14).

To prove the uniqueness, let us set

$$f(\beta) = \delta_a(\beta) + h(\beta) \ ,$$

where $h(\beta)$ is independent of a except for the constraint that $h(\beta) + \delta_a(\beta) \geq 0$. Since $F(\infty) = \int_0^\infty f(\beta)d\beta = 1$, $\int_0^\infty \delta_a(\beta)d\beta = 1$, we have

$$\int_0^\infty d\beta h(\beta) = 0. \tag{2.19}$$

Also, from (2.15) it follows that

$$\beta h(\beta) \to 0 \text{ as } \beta \to 0^+. \tag{2.20}$$

Now

$$f^n(\beta) = \sum_{k=0}^{n} \binom{n}{k} \delta_a^{n-k}(\beta)h^k(\beta).$$

Hence

$$1/n = \sum_{k=0}^{n} \binom{n}{k} \int_0^\infty d\beta\beta^{n-1}\delta_a^{n-k}(\beta)h^k(\beta)$$

$$= \frac{1}{n} + \int_0^\infty d\beta\beta^{n-1}h^n(\beta) + \sum_{k=1}^{n-1} \binom{n}{k} \int_0^\infty d\beta\beta^{n-1}\delta_a^{n-k}(\beta)h^k(\beta). \tag{2.21}$$

A typical integral on the right in the third term is

$$\int_0^\infty d\beta\beta^{n-1}\delta_a^{n-k}(\beta)h^k(\beta) \ , \ 1 \leq k \leq n-1$$

$$= \int_0^a d\beta\beta^{n-1}h^k(\beta)/a^{n-k} \tag{2.22}$$

If one lets a approach zero from the right, then, in view of (2.20) this integral approaches the limit

$$a^{n-1}h^k(a)/(n-k)a^{n-k-1} \to 0. \tag{2.23}$$

Since in (2.21) $a(>0)$ is arbitrary and $h(\beta)$ is independent of a, (2.23) implies that

$$\int_0^\infty d\beta\beta^{n-1}h^n(\beta) = 0 \tag{2.24}$$

for $n = m$ and $n = m+1$, where m (> 1) is some integer.

Rewriting (2.24) for $n = m$ and $n = m + 1$ we have

$$\int_0^\infty d\beta \beta^{m-1} h^m(\beta) = 0, \tag{2.25}$$

$$\int_0^\infty d\beta \beta^m h^{m+1}(\beta) = 0. \tag{2.26}$$

Using the equations (2.25) and (2.26), one can write

$$\int_0^\infty d\beta \beta^{m-1} h^m(\beta) \left[\beta h(\beta) - 1\right] = 0. \tag{2.27}$$

If $h(\beta) \geq 0$, then from (2.25) and (2.26) it is obvious that $h(\beta) = 0$. Suppose $h(\beta) \leq 0$ for some β and m is odd, then from (2.27) evidently $\beta h(\beta) \geq 1$, i.e. $h(\beta) \geq \frac{1}{\beta}$ which is a contradiction (here $\beta > 0$) unless $h(\beta) = 0$. Suppose $h(\beta) \leq 0$ for some β and m is even, then from (2.27) it is obvious that $\beta h(\beta) \leq 1$, i.e. $h(\beta) \leq 0$. Since m is even it follows from (2.25) that $h(\beta) = 0$. Thus

$$h(\beta) = 0 \text{ for all } \beta \text{ in } (0, \infty). \tag{2.25}$$

This proves that (2.18) is the unique solution of (2.14). It can be easily verified that (2.18) is also a solution for the more general equation (2.13). But, α_i's are quite arbitrary in the domain $(0, 1]$ and the right hand side of (2.13) has no dependence on the α's. Hence (2.18) must also be the unique solution of (2.13).

A note for applications. Consider a technical system A consisting of n independent components. Let X_i $(i = 1, 2, ..., n)$ be the survival time of the ith component. Then $X_{(1)}, X_{(2)}, ..., X_{(n)}$ are the successive failure times. Let $Y_1 = X_1 - X_{(1)}, Y_2 = X_2 - X_{(1)}, ..., Y_n = X_n - X_{(1)}$ and denote by $Y_1', Y_2', ..., Y_{n-1}'$ $n - 1$ variables among $Y_1, Y_2, ..., Y_n$ which do not vanish. It is not difficult to prove that if $X_1, X_2, ..., X_n$ are exponentially distributed i.i.d. random variables with d.f. $F(x) = 1 - \exp(-\lambda x)$, $x \geq 0, \lambda > 0$, then $Y_1', Y_2', ..., Y_{n-1}'$ also are i.i.d. random variables having the same exponential distribution. Let $N(t)$ be the number of failures at time t and $N(0) = 0$. One write $N(t) = k$ iff $X_{(k)} \leq t < X_{(k+1)}$. It is clear that system A will stay at state $N(t) = 0$ for a random time $Y_0' = X_{(1)}$ and after this time system will change its state to $N(t) = 1$. Staying in state $N(t) = 1$ for a random time $Y_{(1)}'$ the system will change its state to $N(t) = 2$ etc. Denoting by $Y_1'', Y_2'', ..., Y_{n-2}''$ $n - 2$ variables among $Y_1' - Y_{(1)}', Y_2' - Y_{(1)}', ..., Y_{n-1}' - Y_{(1)}'$ which do not vanish we can conclude that $Y_1'', Y_2'', ..., Y_{n-2}''$ are i.i.d. with the same exponential distribution etc. It is not difficult to observe that Theorem 1 can be rewritten as follows:

Corollary. Let X_i $(i = 1, 2, ..., n)$ be i.i.d. nonnegative continuous random variables with d.f. $F(x)$. Let Y_i $(i = 1, 2.., n)$ and $Y_1', Y_2', ..., Y_{n-1}'$ are defined as above. Then $F(x) = 1 - \exp(-\lambda x)$, $x \geq 0$ for some $\lambda > 0$ if and only if

$$1 + \sum_{i=1}^{n-1} Y_i' \stackrel{d}{=} 1 + \sum_{i=1}^{n-1} Z_i,$$

for two consecutive values of $n = m$ and $m + 1$, where m (> 1) is some integer and Z_i, $i = 1, 2, ..., n - 1$ are i.i.d. random variables with d.f. $F(x) = 1 - \exp(-\lambda x)$, $x \geq 0, \lambda > 0$.

References

[1] Darling, D. A. (1952). The influence of maximum term in the addition of independent random variables. *Trans. Amer. Math.* Soc. 73, 95-107.

[2] Erdelyi, Magnus, (1954). *Oberhettinger and Tricomi, Tables of Integral Transforms, Bateman Manuscript Project*, Vol. I, McGraw-Hill.

[3] Sneddon, I. N., (1951). *Fourier Transforms*, McGraw-Hill.

[3] Stapleton, J. H. (1963). A characterization of the uniform distribution on a compact topological group, *Ann. Math. Stat.* 34., 319-326.

ÖZET

$X_1, X_2, ..., X_n$ bağımsız ve ayni mutlak sürekli F dağılımına sahip olan rasgele değişkenler olmak üzere $X_{(n)} = \max_{1 \leq i \leq n} X_i$ ve $Y_{(1)} = \sum_{i=1}^{n} \frac{X_i}{X_{(n)}}$ olsun. F in $[0, 1]$ de düzgün dağılım fonksiyonu olması için $Y_{(1)}$ istatistiğine dayalı olarak gerek ve yeter koşul verilmiştir.

İstatistik, Journal of the Turkish Statistical Association
1999, Vol.2, No 3, pp. 153-164

PERIODOGRAMS FOR SEASONAL TIME SERIES WITH A UNIT ROOT

Yılmaz Akdi and David A. Dickey
Department of Statistics, Faculty of Science
Ankara University, 06100, Tandogan-Ankara, TURKEY
Department of Statistics, North Carolina State University,
Raleigh, NC 27695, USA
e-mail: akdi@science.ankara.edu.tr

Abstract

This paper extends the periodogram based unit root tests to the seasonal time series models. The problem of testing for a unit root in seasonal time series is something like testing for multiple unit root. That is, in seasonal time series models, there are repeated unit roots. It is found that the asymptotic distribution of the normalized periodogram ordinate is not affected by the seasonality factor and the same test statistic used for autoregressive time series can be used to test for a unit root for seasonal time series models

1. Introduction

The first priority in seasonal modeling is to specify correct differencing and appropriate transformations. The potential behavior of autocorrelation functions for seasonal models is not easy to characterize. The autocovariance function for a seasonal process is quite complicated. To identify a seasonal model from the sample autocorrelation function of the data, first we find d and D so as to make the differenced observations $X_t = (1-B)^d(1-B^s)^D Y_t = \nabla^d \nabla_s^D Y$ stationary. Next

we examine the sample autocorrelation and partial autocorrelation functions of X_t at lags which are multiples of s in order to identify the orders of the model. If $\widehat{\rho}(.)$ is the autocorrelation function of X_t then the orders p and q should be chosen so that $\widehat{\rho}(ks), k = 1, 2, 3, ...,$ is compatible with the autocorrelation of an $ARMA(p, q)$ process. The orders p and q are then selected by attempting to match $\widehat{\rho}(1), \widehat{\rho}(2), ..., \widehat{\rho}(s-1)$ with the autocorrelation function of an $ARMA(p, q)$ process. Ultimately the AIC criterion and the goodness of fit test are used to identify the best Seasonal Aotoregressive Integrated Moving Average (SARIMA) model among competing alternatives. For autoregressive time series the partial autocorrelation function cuts off after some lags and the autocorrelation function decays exponentially but the rate of the decay is important. And for moving average processes, the partial autocorrelation function decays and the autocorrelation function cuts off after some lags. However, for some time series models, the autocorrelation function may be sinusoidal. Consider the model

$$y_t - \mu = \rho(y_{t-12} - \mu) + e_t$$

where e_t is a sequence of uncorrelated random variables with mean zero and constant variance (white noise). This model is applied to monthly data and expresses this December's y, for example, as μ plus a proportion of last December's deviation from μ. If $\mu = 100$, $\rho = 0.8$, and last December's $y = 120$, the model forecasts this December'sy as 100+0.8(20)=116. The forecast for next December's y is 100+.64(20), and the forecast for k Decembers ahead is $100+(0.8)^k(20)$. The model responds to change in the series because it uses only the most recent December to forecast the future. Suppose we allow ρ to be 1 in the AR seasonal model. Then the model is nonstationary and reduces to $y_t = y_{t-12}+e_t$. This model uses last December's y as the forecast for next December (and for any other future December). The difference $y_t - y_{t-12}$ is stationary (white noise). Trend and seasonality are usually detected by inspecting the graph of the (possibly transformed) series. However, they are also characterized by sample autocorrelation functions which are slowly decaying and nearly periodic respectively. Periodograms are usually used to detect periodic components in time series models. Periodograms are also used to estimate the spectral density function.

In this paper we are interested in testing for a unit root in seasonal time series models. Many testing methods have been proposed to test for a unit root in the auto regressive time series models and in the seasonal time series models. The problem arising in many time series applications is the question of whether a series

should be differenced; this is related to asking if the time series has a unit root. Let $\{X_t : t = 1, 2, 3, ...\}$ be a first order autoregressive process defined by

$$X_t = \rho X_{t-1} + e_t, \quad X_0 = 0$$

where $\{e_t : t = 1, 2, 3, ...\}$ is a sequence of independent and identically distributed random variables with $E(e_t) = 0$, and $Var(e_t) = \sigma^2 < \infty$. Let $\widehat{\rho}_n := \left(\sum X_{t-1}^2\right)^{-1} \sum X_t X_{t-1}$ be the least squares estimator of ρ based on the sample of n observations $\{X_1, X_2, ..., X_n\}$. The limit distribution of $\widehat{\rho}_n$ is different for the cases: stationary, unstable and explosive. It is normal for the stationary case and nonnormal for the two nonstationary cases. For instance, in the unstable case, $\rho = 1$, it is known that

$$Z_n := \frac{1}{\sigma}\left(\sum_{t=1}^{n} X_{t-1}^2\right)^{-1/2} (\widehat{\rho}_n - 1)$$

converges weakly to

$$Z := \frac{1}{2}\{W^2(1) - 1\}\left(\int_0^1 W^2(t)dt\right)^{-\frac{1}{2}}$$

as $n \to \infty$, where $\{W(t)\}$ is the standard Browian Motion on $[0, 1]$. Dickey and Fuller (1979) give a representation for the limiting distribution of $n(\widehat{\rho}_n - 1)$. Tables for the percentiles of the distribution can be found in Fuller (1976, pp. 371-3). Dickey, Hasza and Fuller (1984) also give a testing procedure to test for a unit root in seasonal time series. Note that the stationarity of autoregressive time series depends on the roots of the characteristic equation and for seasonal time series, if there is a unit root, then there are more than one unit root. For example, consider the time series model $y_t = \rho y_{t-2} + e_t$ the corresponding characteristic equation is $m^2 - \rho = 0$. If $\rho = 1$ then $m = \pm 1$ are both roots of the equation. Akdi and Dickey (1998) use a periodogram ordinate to test for a unit root. They derive the exact distribution of the normalized periodogram ordinate for the first order auto regressive time series with a unit root. For the higher order time series, they show that the limiting distribution of the normalized periodogram ordinate remains unchanged. They also give the percentiles of the distribution under the assumption $\rho = 1$. In this study, the periodogram based testing procedure has

been extended to seasonal time series with a unit root time series models. It has been shown that limiting distribution remains same for seasonal time series so that same testing procedure developed for first order time series models can be applied to seasonal time series models.

2. The Periodogram Ordinate

The periodogram ordinate is used in many statistical inference problems such as estimating the spectral density function, testing for the presence of a sinusoid with specified frequency, testing for the presence of a Non-Sinusoidal periodic component with specified integer-valued period, and testing for hidden periodicities of unspecified frequency. Spectral analysis for time series, in particular the estimation of the spectral density function, depends heavily on the asymptotic distribution as $n \to \infty$ of the periodogram ordinates of the series $\{X_1, X_2, ..., X_n\}$. Here, our purpose is to use the periodogram ordinate to test for a unit root in a seasonal time series based on the sample. For stationary time series, there is a one-to-one relationship between the autocorrelation function of the time series and the spectral density function by using the Fourier transformation. However, when $\rho = 1$ there is no autocovariance function and hence the spectral density function can not be defined as a Fourier transform of the autocovariance function. But by using the distributional properties derived in this paper, one can define the spectral density function at frequencies near zero.

Periodograms are often used for studying periodic behavior in data. They decompose the variation in data into periodic components . Basic distributional properties of the periodogram ordinates are assumed to be understood. Akdi (1995) studies the distributional properties of the periodogram ordinates for autoregressive time series with a unit root. Akdi and Dickey (1998) give a testing methodology to test for a unit root by using the periodogram ordinates. In this study, a seasonal time series with a unit root satisfying

$$(Y_t - \mu) = \rho(Y_{t-d} - \mu) + e_t, \quad t = 1, 2, 3, ..., n \tag{1}$$

is considered with appropriate starting values and e_t are assumed to be uncorrelated with mean 0 and variance σ^2. Note that the process is stationary if $|\rho| < 1$. For such a time series, forecasts tend eventually to the sample mean, and standard estimators of ρ and μ converge to a normal distribution. If $\rho = 1$ in (1) and if

$Y_0 = \mu$ the forecasts are not mean reverting and the usual estimators of ρ are nonnormal in the limit. Note that μ drops out of (1) if $\rho = 1$. Consider the model in (1) with $\rho = 1$

$$Y_t = Y_{t-d} + e_t, \quad t = 1, 2, 3, ..., n$$

The periodogram ordinate of Y_t is defined as

$$I_n(w_k) = \frac{n}{2}\left(a_k^2 + b_k^2\right) \tag{2}$$

where a_k and b_k are known as Fourier coefficients of the time series defined by

$$a_k = \frac{2}{n}\sum_{t=1}^{n}(Y_t - \mu)\cos(w_k t), \qquad b_k = \frac{2}{n}\sum_{t=1}^{n}(Y_t - \mu)\sin(w_k t) \tag{3}$$

If μ is unknown, then μ can be replaced with the sample mean. But when $w_k = 2\pi k/n$, $k = 1, 2, 3, ...[n/2]$ then $\sum_{t=1}^{n}\cos(w_k t) = \sum_{t=1}^{n}\sin(w_k t) = 0$; and hence the Fourier coefficients a_k and b_k have mean zero when Y_t has a constant expected value. Here, $[n/2]$ denotes the largest integer less than $n/2$. The purpose is to find the distribution of the periodogram ordinate defined in (2) and thus the problem reduces to find the joint distribution of the Fourier coefficients a_k and b_k under the assumption $\rho = 1$. Note that the periodogram ordinate is a smooth function of a sum of e_j's therefore, we can use our results as an approximation as long as e_t satisfies assumptions of Donsker's theorem and n is large enough. Therefore, we can assume that errors are independent and normally distributed random variables with mean zero and variance σ^2.

Consider the time series

$$(Y_t - \mu) = \rho(Y_{t-1} - \mu) + e_t, \quad t = 1, 2, 3, ..., n.$$

when $|\rho| < 1$ then the normalized periodogram ordinate is asymptotically distributed as chi-square with 2 degrees of freedom. That is,

$$\frac{I_n(w_k)}{f(w_k)} \xrightarrow{D} \chi_2^2, \quad \text{as } n \to \infty \text{ where } f(w_k) = \frac{\sigma^2}{1 + \rho^2 - 2\rho\cos(w_k)} \tag{4}$$

and when $\rho = 1$, Akdi and Dickey (1998) show that the normalized periodogram ordinate is distributed as mixture of chi-squares with one degree of freedom each. That is, for the first order auto regressive time series

$$\frac{I_n(w_k)}{f(w_k)} \sim Z_1^2 + 3Z_2^2, \quad \text{where } f(w_k) = \frac{\sigma^2}{2(1 - 2\cos(w_k))} \tag{5}$$

where (Z_1, Z_2) is a pair of independent standard normals and for a general ARMA(p,q) processes

$$\frac{4\pi^2 k^2}{\sigma^2 \phi^2} I_n(w_k) \xrightarrow{D} Z_1^2 + 3Z_2^2 \text{ as } n \to \infty \tag{6}$$

Notice that the low frequency periodogram ordinates are small for stationary time series and large for nonstationary series (variance increases over time for nonstationary case). A test statistic

$$T_n(w_1) = \frac{2(1 - \cos(w_1))}{\widehat{\sigma}_n^2} I_n(w_1) \tag{7}$$

can be used to test the null hypothesis $H_0 : \rho = 1$ against stationary alternatives because the distribution of the test statistic is known under both null and alternative hypothesis. The critical values of the null distribution can be found in Akdi and Dickey (1998). Our goal is to show that the same testing procedure can be used to test for a unit root in the seasonal time series with a unit root.

3. Distribution of the Periodogram Ordinate for Seasonal Time Series

Consider the time series given in (1) with $\rho = 1$. The Fourier coefficients defined in (3) can be written as a sum of independent random variables.

$$a_k = a_{1,k} + a_{2,k} + ... + a_{d,k} \quad , \quad \text{and} \quad b_k = b_{1,k} + b_{2,k} + ... + b_{d,k} \tag{8}$$

here

$$a_{i,k} = \frac{2}{n} \sum_{t=1}^{n} Y_{i,dt-i+1} \cos(w_k(dt - i + 1)), \; b_{i,k} = \frac{2}{n} \sum_{t=1}^{n} Y_{i,dt-i+1} \sin(w_k(dt - i + 1))$$

such that $a_{i,k}, a_{j,k}, b_{i,k}, b_{j,j}$ and $a_{i,k}, b_{j,k}$ are all independent for all $i \neq j$.

For simplicity let us take $d = 2$. Then $Y_t = Y_{t-2} + e_t$ where e_t is a sequence of independent and identically distributed random variables with mean 0 and

variance σ^2. $Y_{1,t} = e_1 + e_3 + e_5 + ... + e_{d(t-1)}$ and $Y_{2,t} = e_2 + e_4 + e_6 + ... + e_{dt}$. In general,

$$Y_{i,t} = \sum_{j=0}^{t-1} e_{i+dj} = e_i + e_{i+d} + e_{i+2d} + ... + e_{i+d(t-1)}$$

Notice that the random variables $Y_{1,t}$ and $Y_{2,t}$ are independent and thus the Fourier coefficients related to $Y_{1,t}$ and $Y_{2,t}$ are independent. The problem is to find the distribution of the normalized periodogram ordinate which is defined in terms of the Fourier coefficients a_k and b_k. Thus we need to find the joint distribution of the Fourier coefficients. Notice that $(a_k, b_k)' = \mathbf{AX}$ where

$$\mathbf{A} = \begin{bmatrix} 1 & 0 & 1 & 0 & 1 & . & . & . & 1 & 0 \\ 0 & 1 & 0 & 1 & 0 & . & . & . & 0 & 1 \end{bmatrix}_{2\times 2d},$$

$$\mathbf{X} = (a_{1,k}, b_{1,k}, a_{2,k}, b_{2,k}, ..., a_{d,k}, b_{d,k})'$$

In order to find the distribution of $\mathbf{AX}$, it is enough to find the joint distribution of $(a_{i,k}, b_{i,k})'$ and since they are normally distributed random variables, we only need to calculate its mean vector and the variance-covariance matrix of $\mathbf{AX}$. Obviously, the mean vector is the zero vector. The variances can be calculated as

$$Var(a_{i,k}) = \frac{4\sigma^2}{n^2} \sum_{t=1}^{n} \sum_{s=1}^{n} \left\{ \min(dt - i + 1, ds - i + 1) \cos\left(2\pi k \frac{dt-i+1}{n}\right) \right.$$
$$\left. . \cos\left(2\pi k \frac{ds-i+1}{n}\right) \right\}$$

$$= 4n\sigma^2 \sum_{t=1}^{n} \sum_{s=1}^{n} \left\{ \min\left(\frac{dt-i+1}{n}, \frac{ds-i+1}{n}\right) \cos\left(2\pi k \frac{dt-i+1}{n}\right) \right.$$
$$\left. . \cos\left(2\pi k \frac{ds-i+1}{n}\right) \left(\frac{1}{n}\right)^2 \right\}$$

Note that for fixed k, this double sum can be approximated as a double integral and after some calculations and using the trigonometric identities we get

$$\frac{1}{n} Var(a_{i,k}) \to 4\sigma^2 d \int_0^1 \int_0^1 \min(x, y) \cos(2\pi k dx) \cos(2\pi k dy) \partial x \partial y = \frac{\sigma^2}{2\pi^2 k^2 d}.$$

(Here, to avoid notational confusion ∂ is used to indicate the differential). When $Var(b_{i,k})$ and $Cov(a_{i,k}, b_{i,k})$ are calculated similarly

$$\frac{1}{n}Var(b_{i,k}) \to 4\sigma^2 d \int_0^1 \int_0^1 \min(x,y)\sin(2\pi k dx)\sin(2\pi k dy)\partial x \partial y = \frac{3\sigma^2}{2\pi^2 k^2 d}$$

and

$$\frac{1}{n}Cov(a_{i,k}, b_{i,k}) \to 4\sigma^2 d \int_0^1 \int_0^1 \min(x,y)\cos(2\pi k dx)\sin(2\pi k dy)\partial x \partial y = 0$$

Thus,

$$\frac{1}{\sqrt{n}}\begin{bmatrix} a_{i,k} \\ b_{i,k} \end{bmatrix} \xrightarrow{D} N(0, V_1^*) \text{ , as } n \to \infty \quad \text{where } V_1^* = \frac{\sigma^2}{2\pi^2 k^2 d}\begin{bmatrix} 1 & 0 \\ 0 & 3 \end{bmatrix} \tag{9}$$

But we want to find the distribution of $(a_k, b_k) = \mathbf{AX}$. First of all, the asymptotic distribution of $\mathbf{X}/\sqrt{n}$ is also normally distributed with mean $\mathbf{0}$ vector and variance covariance matrix $\mathbf{V}_1$ where $\mathbf{V}_1$=diag$\{\mathbf{V}_1^*, \mathbf{V}_1^*, ..., \mathbf{V}_1^*\}$. Thus using the fact that all the components of $\mathbf{X}$ are independent ($a_{i,k}, a_{j,k}, b_{i,k}, b_{j,j}$ and $a_{i,k}, b_{j,k}$ independent for all $i \neq j$) we can calculate the variance-covariance matrix of (a_k, b_k). The asymptotic distribution of $(a_k, b_k) = \mathbf{AX}$ is normal with mean vector $\mathbf{0}$ and variance covariance matrix $\mathbf{V} = \mathbf{AV_1A'}$. The resulting variance-covariance matrix is invariant to the seasonality factor d and thus the asymptotic distribution is also free from the seasonality factor d.

$$\mathbf{V} = \mathbf{AV_1A'} = \frac{\sigma^2}{2\pi^2 k^2}\begin{bmatrix} 1 & 0 \\ 0 & 3 \end{bmatrix} \tag{10}$$

Hence,

$$\frac{1}{\sqrt{n}}\begin{bmatrix} a_k \\ b_k \end{bmatrix} \xrightarrow{D} N(\mathbf{0}, \mathbf{V}) \text{ , as } n \to \infty$$

This implies that

$$\frac{1}{\sqrt{n}}(a_k, b_k)\frac{1}{\sqrt{n}}\begin{pmatrix} a_k \\ b_k \end{pmatrix} = \frac{1}{n}(a_k^2 + b_k^2) \xrightarrow{D} \frac{\sigma^2}{2\pi^2 k^2}\left(Z_1^2 + 3Z_2^2\right), \text{ as } n \to \infty$$

or

$$\Rightarrow \frac{2\pi^2 k^2}{n\sigma^2}\left(a_k^2 + b_k^2\right) \xrightarrow{D} Z_1^2 + 3Z_2^2, \text{ as } n \to \infty$$

$$\Rightarrow \frac{4\pi^2 k^2}{n^2\sigma^2}\frac{n}{2}\left(a_k^2 + b_k^2\right) \xrightarrow{D} Z_1^2 + 3Z_2^2, \text{ as } n \to \infty$$

$$\Rightarrow \frac{4\pi^2 k^2}{n^2\sigma^2}\frac{n}{2}\left(a_k^2 + b_k^2\right) \xrightarrow{D} Z_1^2 + 3Z_2^2, \text{ as } n \to \infty$$

$$\Rightarrow \left(\frac{2\pi k}{n}\right)^2 \frac{1}{\sigma^2} I_n(w_k) = \frac{w_k^2}{\sigma^2} I_n(w_k) \xrightarrow{D} Z_1^2 + 3Z_2^2, as n \to \infty$$

or

$$\frac{I_n(w_k)}{f(w_k)} \xrightarrow{D} Z_1^2 + 3Z_2^2, \text{ as } n \to \infty$$

For fixed k,

$$\frac{2(1-\cos(w_k))}{w_k^2} \to 1, \text{ as } n \to \infty$$

which implies that

$$\frac{2(1-\cos(w_k))}{\sigma^2} I_n(w_k) \xrightarrow{D} Z_1^2 + 3Z_2^2, \text{ as } n \to \infty$$

Therefore we can use the same test statistic given in (7) to test for a unit root in seasonal time series.

4. Example: Testing for Stationarity

In this section, we will try to test the null hypothesis $H_0 : \rho = 1$ against stationary alternatives in the model $y_t = \rho y_{t-4} + e_t$. Note that the value of the periodogram ordinate at the low frequencies is large for time series with unit root and small for stationary time series. And thus, the value of the test statistics is

large for nonstationary time series and small for stationary time series. Therefore, we reject the null hypothesis of unit root if $T_n(w_k)$ is small. Even though, this testing procedure is valid for any k, it is better to use small k's; e.g. $k = 1$. The tables for the critical values are available from Akdi and Dickey (1998).

For an illustration we generate 100 observations from a seasonal time series with a unit root: $y_t = y_{t-4} + e_t$ where e_t is a sequence of independent normally distributed random variables with mean 0 and variance 1. From identification plots (the autocorrelations and partial autocorrelations), we see that the decay of the autocorrelations are very slow and the seasonality factor seems to be 4. By regressing y_t on y_{t-4} we calculate an estimate of variance; σ_n^2 =1.0867 and using SAS's proc spectra, we calculate the first periodogram ordinate $I_n(w_1) = 274.56$ The value of the test statistic ($T_n(w_1)$) is 0.99711 According to the rule, we reject the null hypothesis of unit root at α=0.05 if $T_n(w_1) < 0.178$. And thus, we fail to reject the null hypothesis at 5% level. Table 1 summarizes some other values of the test statistics.

Same procedure is repeated for a stationary seasonal time series $y_t = 0.8y_{t-4} + e_t$ where e_t is a sequence of independent normally distributed random variables with mean zero and variance 1. From identification plots (the autocorrelations and partial autocorrelations), we see that the decay of the autocorrelations are very fast and seasonality factor seems to be 4. The value of the first periodogram ordinate is 1.60598 and the value of the test statistic is 0.005244 which is smaller that the 5% critical value 0.178 so that we reject the null hypothesis of a unit root.

Table 1. Values of the Test Statistics

	ρ=1	$\rho = 1$	%5 Critical Value	ρ=0.8	ρ=0.8
k	1	4		1	4
Freq.	0.06283	0.25133	0.178	0.06283	0.25133
$I_n(w_k)$	274.56	17.924	0.178	1.60598	2.47794
$T_n(w_k)$	0.99711	1.03638	0.178	0.00524	0.1289
	Fail to Reject H_0	Fail to Reject H_0		Reject H_0	Reject H_0

Some other critical values of the test statistics are summarized in Table 2 which can be used for calculation of the powers.

Table 2. Percentiles of $Z_1^2 + 3Z_2^2$ (Z_i independent $N(0,1)$)

α	0.001	0.01	0.025	0.05	0.10	0.20	0.50	0.80	0.90	0.95	0.975	0.99
z	.0035	.0348	.088	.178	.368	.79	2.54	6.32	9.48	12.85	16.37	21.17

Conclusion

In this study, the distribution of the periodogram ordinates of seasonal time series with a unit root has been derived. Using the distributional properties of the periodogram ordinate under the null and alternative hypothesis have been discussed and it is shown that the testing procedure given in Akdi and Dickey (1998) can be applied to the seasonal time series with a unit root. For an illustration, two data sets generated from a seasonal time series are discussed.

References

[1] Akdi, Y. (1995), *Periodogram Analysis for Unit Roots*, Ph.D. Thesis, North Carolina State University.

[2] Akdi, Y. and D. A. Dickey (1998) *Periodogram of Unit Root Time Series: Distribution and Tests*, Communications in Statistics: Theory and Methods,Vol. 27, 69-87

[3] Box, G. E. P., G. M. Jenkins and G. C. Reinsel (1994), *Time Series Analysis, Forecasting and Control*, Prentice Hall, Inc.

[4] Broclebank, J.C. and D.A.Dickey (1986) *SAS System for Forecasting Time Series*, SAS Institute

[5] Brockwell, P.J. and R.A. Davis (1987) , *Time Series: Theory and Methods*, Springer-Verlag New York Inc.

[6] Dickey, D.A. and W.A. Fuller (1979), *Distribution of Estimators for Autoregressive Time Series with a Unit Root*, JASA, 74, 427-431

[7] Dickey, D.A., D.P. Hasza, and W.A. Fuller (1984), *Testing for Unit Roots in Seasonal Time Series*, JASA, 79, 355-367

[8] Fuller, W.A. (1976), *Introduction to Statistical Time Series*, Wiley, New York.

ÖZET

Bu çalışma periodogram ile yapılan birim kök testlerini mevsimsel zaman serilerine genişletmektedir. Birim köklü mevsimsel zaman serilerinde birim kökler tekrar etmektedir. Burada gösterilmiştir ki, birim köklü AR serileri için elde edilen normalleştirilmiş periodogramların asimptotik dağılımları birim köklü mevsimsel zaman serileri için de aynıdır.

İstatistik, Journal of the Turkish Statistical Association
1999, Vol.2, No 3, pp. 165-174

PROCESS PERFORMANCE MEASURES WHEN PROCESS DISTRIBUTION IS NON-NORMAL

Donald S. Holmes
Stochos Inc. 14 N. College Street Schenectady, N.Y. 12305 U.S.A.
A. Erhan Mergen
Rochester Institute of Technology College of Business,
Decision Sciences 107 Lomb Memorial Drive Rochester,
N.Y. 14623-5608 U.S.A.

Abstract

This paper addresses the problems associated with process performance measures, such as Cp, Cpk, when the frequency distribution of the variable being evaluation is not Normal. These measures, also known as capability indices, are commonly used in industry, yet they may not reflect the true process performance if the process distribution is not Normal. Gunter (1), in his four-part series articles, emphasized this point and other problems associated with measures like Cpk. In this paper, we discuss various scenarios with respect to process stability and frequency distribution, and provide an example using non-Normal process curve.

1. Introduction

There are some processes for which the data is not expected to be Normally distributed, for example, plating, drilling, etc. operations. When this situation occurs, some non-Normal frequency curve is used to fit the data. This activity is usually undertaken for one of two reasons:

1. Making X control charts because of low rates of data accumulation or
2. Calculation of the process performance measures (Cp, Cpk, etc.)

The use of X charts should not be an issue since there are several charts which allow the plotting of each data point that have much better average run lengths and are not nearly as sensitive to non-Normality of the data. These charts include the

Cumulative Sum (Cusum), the Exponentially Weighted Moving Average (EWMA) and the Dynamic Histogram charts (see, for example, Montgomery (2), and Holmes and Mergen (3) for these charts.)

This paper addresses non-Normality problems with respect to the second issue: process performance measures. For definitions of these measures, please consult Gitlow, Oppenheim and Oppenheim (4), for example.

DISCUSSION

Capability vs. Performance:

Let's concentrate on the performance measure, which deals with the width of a process relative to the allowed (tolerance) width. This measure is defined as:

$$\frac{USL - LSL}{Process\ Width} \tag{1}$$

where USL and LSL stand for the upper and lower specification limit, respectively.

The process width used in the equation above can be one of two possibilities:

1. The width of the process as it exists -the *performance* width - or
2. The width of the process as it could be if the process were in control - the *capability* width.

The relative width measure is referred to as the Pp in the first case and the Cp in the second case. Note that the term Cp is reserved for processes, which are in control, i.e., statistical control (the process is said to be in statistical control when it is influenced only by common causes of variation).

If the process is not in control, the capability width may be significantly smaller in magnitude than the performance width. This causes differences, of course, in the reported process performance measures.

Normal Process:

If the frequency curve is approximately Normal, the width is usually taken to be ± 3 standard deviations around the average. The *performance* standard deviation is the one calculated for the entire data set without regard as to whether or not the data gave evidence of lack of statistical control. The *capability* standard deviation, on the other hand, is one, which is independent of chances in average values. It can be obtained from control chart calculations such as $\overline{R}/d2$ or $\overline{s}/c4$, where $\overline{R}$ and $\overline{s}$ are the average of the subgroup ranges and the average of the subgroup standard deviation, respectively. The values of $d2$ and $c4$ can be read from tables for control chart constants for a given subgroup size. Another method for calculating the *capability* standard deviation is the mean square successive difference (MSSD) (see Holmes and Mergen (5) Hald(6), for example). Using MSSD, the capability standard deviation would be estimated as follows:

$$\sigma_{MSSD} = \sqrt{\frac{MSSD}{2}} \tag{2}$$

where

$$MSSD = \frac{1}{(n-1)} \sum_{i=1}^{n-1} (X_{i+1} - X_i)^2 \tag{3}$$

and X_i are the individual observations, n is the number of observations.

Roes, Does Schuring (7), gave the unbiased estimate of the standard deviation using MSSD as

$$= \frac{\sqrt{\sigma_{MSSD}}}{1 - \frac{3}{8n}} \tag{4}$$

which will converge rapidly to the expression given in equation (2) as n gets large.

Non-Normal and Stable (i.e., In-Control) Process:

If the process follow a non-Normal distribution, then the width of the curve is determined by fitting a non-Normal curve to the data. Once the curve is fitted, the width may be determined by calculating the values of the variable, which include 99.7% of the data. The minimum X is usually taken to be the one which has 0.15% below it; the maximum X is taken to be the one which has 0.15% above it. The process width is taken to be $X_{\max} - X_{\min}$.

Problem#1: The curve type used in fitting the data impacts on the estimate of the process width.

The curve type selected is subjective and one can only reject unfit curves, not guarantee the selection of the "right" curve, so consistent results must be based on a standardized curve fitting approach. We think to get a consensus on this matter will be very difficult.

Problem#2: For every curve expect the Normal the average and standard deviation are not independent.

Thus striving for centering the process on nominal value will also change the width of the process, which is used in the denominator of Cp and Cpk type measures. For example, assume we have fitted Rayleigh distribution to a non-Normal process data (see Appendix I for a description of the Rayleigh distribution). The process average ($\overline{X}$) and target (T) (i.e., nominal) are given as

$\overline{X} = 5$, and $T = 10$, respectively. From equation (4) and (8) in Appendix I, the standard deviation can be estimated as

$$s = (1.1284)(0.4633)\overline{x} \tag{5}$$

As you see in the above equation, if the average is moved to be closer to the target, the standard deviation will get larger and have a direct impact on the Cp. Thus improving one quality index automatically worsens another.

Non-Normal and Unstable (i.e., not In-Control) Process:

Fitting a curve to an unstable process is inherently dangerous. Should the issue of stability (control) be ignored when fitting a non-Normal curve to the data, then incorrect conclusions relative to the quality level may occur.. The example below demonstrates this point in the context of the Rayleigh distribution.

Problem#3: If the process is not in control (i.e., not stable), then estimation of curve parameters that depend on the average will not be reasonable since the average does not reflect the changes in process.

In other words, using the average ($\overline{X}$) to estimate the value for curve parameter does not allow one to distinguish between the capability and the performance of the process. However, there are ways to calculate the standard deviation that will enable the distinction between capability and performance to be made. The standard deviation estimated through MSSD provides a method to distinguish between capability and performance (see, for example, Holmes and Mergen (5)).

EXAMPLE

Consider the histogram and the descriptive statistics summary obtained recently from a process (see Figure 1 and Table 1) which is known to generate an approximate Rayleigh distribution. The complete data set is listed in Appendix II.

(Approximate location for Figure 1 and Table 1)

It is clear from the histogram that the data is not Normally distributed (a chi-square test also rejected Normality). The specification limits for the variable in question (i.e., quality characteristic) are:

$USL = 5.00$ $Nominal = 3.00$ $LSL = 1.00$

During the time period in which the data is collected, the regular standard deviation (σ_R) is 1.102 and the mean square successive difference (MSSD) standard deviation (σ_{MSSD}) is 0.595. The two variance are significantly different as per the Z test described in Dixon and Massey (8). This means, in turn, that the process is not in control. This is also evident from the X-bar chart shown in Figure 2 (for subgroup size five).

(Approximate location for Figure 2)

Thus, in turn, there will be a significant difference between the Cp and the Pp for this process. The process performance calculations based on process width estimated with the Rayleigh distribution using the mean, the regular, and also the MSSD standard deviations are shown in the table below (Table 2).

(Approximate location for Table 2)

The Cp of 1.24 is an indication of what the process is capable of doing if it were to be brought into control, whereas the Pp (0.428 or 0.667 depending on which estimate of q is used) indicates how well the process is currently performing. The difference between these estimates is significant and points out the potential problem mentioned above in estimating performance measures from a curve fitted to data from an unstable (i.e., not in control) process.

CONCLUSION

This paper demonstrates that the use of process performance indices for non-Normal data is subject to many problems. Problem 1 is solvable by everyone agreeing to a specific family of curves. Problem 2 cannot be resolved. Problem 3 calls for careful analysis before fitting the curve. But, problem 2 indicates the only meaningful result may be to give up Cp, Cpk, etc. and go back to the more universally accepted percent defective or parts per million (ppm) plus a measure of how far the process center is from the nominal.

KEY WORDS: Non-Normal process distribution, process performance measures.

REFERENCES

[1] Gunter, B.H. (1989)."The Use and Abuse of Cpk,"Part 1-4, *Quality Progress,* Vol.**22**, No.s1,3,5,7.

[2] Montgomery, D.C. (1991). *Introduction to Statistical Quality Control,* second edition, Wiley, New York, pp.280-399.

[3] Holmes, D.S. and Mergen, A.E. (1990). "The Dynamic Histogram Chart," *Quality and Reliability Engineering, International,* Vol.**6**, No.2, pp.107-111.

[4] Gitlow, H. Oppenheim, A. and Oppenheim, R. (1995). *Quality Management: Tools and Methods for Improvement,* Irwin, Boston, pp.352-387.

[5] Holmes, D.S. and Mergen, A.E. (1993). "Improving the Performance of the T^2 Control Chart," *Quality Engineering,* Vol.**5**, No.4, pp.619-625.

[6] Hald, A. (1967). *Statistical Theory with Engineering Applications,* John Wiley and Sons, New York, pp.357-360.

[7] Roes, K.C.B. Does, R.M.M. and Schuring, Y. (1993). "Shewhart-Type Control Charts for Individual Observations," Journal Of Quality Technology, Vol..**25**, No.3, pp.188-198.

[8] Dixon, W.J. and Massey, F.J. (1977). *Introduction to Statistical Analysis,* Richard D. Irwin, pp.353-354.

[9] Nelson, W. (1982). *Applied Life Data Analysis,* John Wiley and Sons, New York, p.36-37.

APPENDIX I

Rayleigh Distribution:

The Rayleigh distribution is a special case of Weibull where the shape parameter, β, is equal to 2 (Nelson (9)). The probability density function for the Rayleigh curve is:

$$f(x) = (\frac{2}{q^2})xe^{-(\frac{x}{q})}dx^2 \tag{6}$$

The curve is usually fitted using the average of the data to find the value for q (the "scale" parameter) as shown below.

$$E(X) = q\Gamma(\frac{3}{2}) = q\frac{\sqrt{\pi}}{2} \tag{7}$$

where Γ represents gamma function and $\pi = 3.141593$.

Hence the value of the scale parameter is usually estimated using:

$$q = \frac{2\overline{x}}{\sqrt{\pi}} = 1.1284\overline{x} \tag{8}$$

This value for q is then used to determine the value of x which has 0.15% of the curve below it ($X_{\min}$) and the value of x which has 0.15% of the data above it ($X_{\max}$). The values for $X_{\max}$ and $X_{\min}$ may be calculated as:

$$x_{\max} = q\sqrt{-\ln 0.0015} = 2.54996q \tag{9}$$

$$x_{\min} = \sqrt{-\ln 0.9985} = 0.03874q \tag{10}$$

The variance for the Raleigh distribution, on the other hand, is:

$$V(X) = q^2[\Gamma(2) - \Gamma(\frac{3}{2})^2] \tag{11}$$

and the standard deviation, s, would be

$$s = 0.4633q \tag{12}$$

Hence the value of the scale parameter may also be obtained using:

$$q = 2.1584s \tag{13}$$

Once expressed in this fashion, one can distinguish between the capability and performance distribution using the appropriate standard deviation mentioned above. The capability estimate of s may be obtained using $\overline{R}/d_2$ or MSSD as mentioned earlier.

APPENDIX II

1.	2.17	51.	2.62	101.	3.60	151.	4.44
2.	3.53	52.	2.35	102.	2.57	152.	4.52
3.	2.62	53.	2.07	103.	3.07	153.	4.35
4.	2.53	54.	3.08	104.	3.49	154.	4.33
5.	2.18	55.	3.49	105.	2.43	155.	4.87
6.	3.13	56.	2.88	106.	4.47	156.	4.92
7.	3.18	57.	3.13	107.	2.15	157.	4.00
8.	3.60	58.	2.97	108.	3.96	158.	5.55
9.	2.09	59.	2.48	109.	2.68	159.	4.11
10.	2.10	60.	2.47	110.	3.02	160.	5.63
11.	2.08	61.	3.84	111.	3.33	161.	4.97
12.	2.62	62.	2.42	112.	2.51	162.	5.21
13.	2.45	63.	2.76	113.	3.06	163.	5.35
14.	2.49	64.	2.40	114.	2.10	164.	4.97
15.	3.35	65.	3.21	115.	2.15	165.	4.06
16.	2.70	66.	2.16	116.	4.42	166.	4.69
17.	2.92	67.	2.77	117.	4.03	167.	5.13
18.	2.59	68.	2.23	118.	3.47	168.	4.38
19.	2.48	69.	3.95	119.	2.81	169.	4.50
20.	2.69	70.	2.07	120.	2.67	170.	5.44
21.	3.01	71.	3.20	121.	2.09	171.	4.46
22.	2.74	72.	2.89	122.	2.20	172.	5.66
23.	2.01	73.	2.58	123.	2.57	173.	5.83
24.	2.81	74.	2.34	124.	4.80	174.	5.06
25.	2.22	75.	2.98	125.	2.64	175.	5.46
26.	2.09	76.	2.22	126.	2.53	176.	5.31
27.	3.19	77.	2.60	127.	2.59	177.	5.28
28.	2.29	78.	2.50	128.	2.65	178.	5.07
29.	4.06	79.	2.58	129.	2.20	179.	4.05
30.	2.88	80.	2.14	130.	3.80	180.	5.21
31.	3.40	81.	2.65	131.	2.39	181.	6.80
32.	2.94	82.	2.76	132.	3.40	182.	5.36
33.	2.30	83.	2.33	133.	2.11	183.	6.21
34.	2.98	84.	2.57	134.	2.43	184.	4.05
35.	2.07	85.	2.70	135.	2.67	185.	5.30
36.	2.32	86.	2.43	136.	2.22	186.	4.39
37.	2.84	87.	2.53	137.	2.15	187.	4.77
38.	2.22	88.	2.03	138.	3.06	188.	5.96
39.	2.52	89.	3.53	139.	2.08	189.	6.05
40.	2.88	90.	2.30	140.	2.88	190.	4.41
41.	2.66	91.	3.43	141.	2.97	191.	5.07
42.	3.39	92.	3.07	142.	2.98	192.	4.07
43.	3.34	93.	2.23	143.	2.24	193.	4.19
44.	2.34	94.	2.58	144.	2.59	194.	5.16
45.	2.51	95.	2.25	145.	2.86	195.	4.78
46.	2.57	96.	3.16	146.	2.76	196.	4.06
47.	3.19	97.	2.79	147.	2.30	197.	5.17
48.	4.20	98.	2.30	148.	2.62	198.	5.14
49.	2.62	99.	2.53	149.	2.39	199.	4.04
50.	2.88	100.	3.18	150.	2.89	200.	4.09

Figure 1. Histogram of the data.

Table 1. Summary of descriptive statistics of the data.

Figure 2. $\overline{X}$ and Range charts of the data.

Table2. Process performance calculations using Rayleigh distribution.

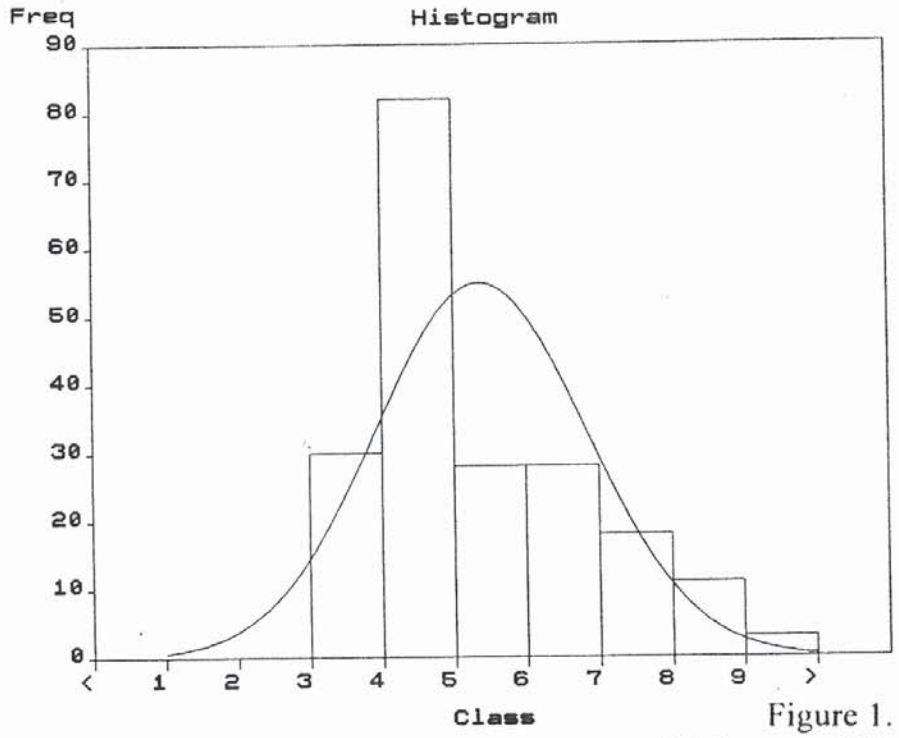

Figure 1.
(Holmes and Mergen)

Mean	= 3.298	Median	= 2.880
Reg. std. dev. (σ_R)	= 1.102	SE Mean	= 0.078
Range	= 4.790	# Observ	= 200
Minimum	= 2.010	Maximum	= 6.800
Skewness	= 0.952	Kurtosis	= 2.855
Cap. SD	= 0.595	Cap. Ratio	= 0.540
Mean Square Successive Difference (MSSD) Tests			
Normal Z	= 10.069	MSSD(SD)	= 0.595

Table 1. Summary of descriptive statistics.

Basis for q	q	Std. Dev.	X_{max}	X_{min}	Width (X_{max} - X_{min})	Relative Width (Pp or Cp)
Performance (using mean)	3.72	*****	9.486	0.144	9.342	0.428 (Pp)
Performance (using regular std. dev.)	2.38	1.102	6.069	0.092	5.977	0.667 (Pp)
Capability (using MSSD std.dev.)	1.28	0.595	3.264	0.049	3.215	1.244 (Cp)

Table 2. Process performance calculations using Rayleigh distribution.

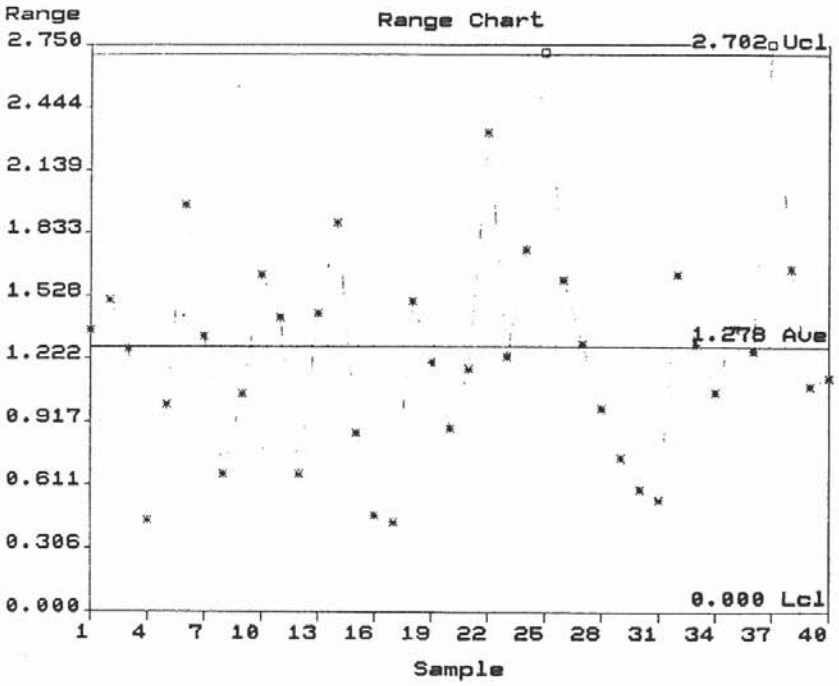

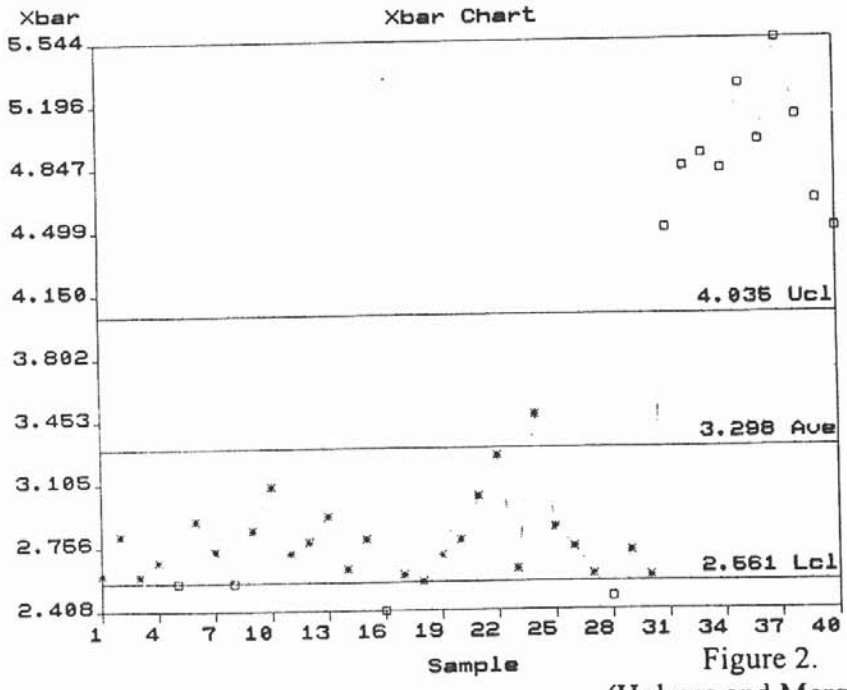

Figure 2.
(Holmes and Mergen)

İstatistik, Journal of the Turkish Statistical Association
1999, Vol.2, No 3, pp. 175-186

THE OPTIMAL CONTROL PROBLEM FOR THE ELLIPTIC EQUATION

Niftiyev A.A. and Gasimov Yu.S.
Baku State University, Department of Mathematics,
Baku, Azerbaijan

Abstract

The general method for optimal control problem for the elliptic equation with unknown border is proposed. This method allows to investigate a large class of problems which are reduced to the finding of the optimal form.

Key Words: Optimal control, elliptic equation, quasidifferential, convex function

1. Introduction

A large class of practical problems - especially problems of theory of elasticity, hydrodynamics, geophysics, aerodynamics and statistical control applications - are reduced to the finding of the optimal form.

In spite of actuality of these problems, their solution consists of some mathematical difficulties. Therefore such problems are solved only in particular cases.

In present work, the general method is proposed, based on the definition of variation of domain and increment of the depending on the domain functional.

This method allows to investigate a large class of such problems and construct effective algorithms for their numerical solution.

2. The main results

Let K be any subset of the class of convex bounded domains D from R^n and $G \in R^n$, is such a bounded convex reserved set, that if $D \in K$, then $D \in G$. Let $S_D \equiv \partial D$.

We consider the following problem:

$$I(D) = \int_D F(x, u(x), u_x(x))\, dx \to \min,\ D \in K, \tag{1}$$

$$\sum_{i,j=1}^{n} (a_{ij}u_{x_i})_{x_j} + a(x)u = f,\ x \in D, \tag{2}$$

$$u(\xi) = g(\xi),\ \xi \in S_D. \tag{3}$$

Here F, f, g, a_{ij}, a are given functions, $a_{ij}(x) = a_{ji}(x)$, $i, j = \overline{1,n}$, $x \in R^n$ and $a_{ij}(x)$ satisfies the condition of uniform ellipticity in the bounded domain $G \in R^n$, i.e.

$$\mu_1 |\xi|^2 \leq \sum_{i,j=1}^{n} a_{ij}\xi_i\xi_j \leq \mu_2 |\xi|^2,\ |\xi|^2 = \sum_{i=1}^{n} \xi_i^2, \tag{4}$$

μ_1, $\mu_2 > 0$ are any constants.

Condition (4) holds for any $\xi = (\xi_1, \xi_2, ..., \xi_n) \in R^n$, $0 < \mu_3 \leq a(x) \leq \mu_4$, $x \in G$.

Let f, g, a and a_{ij}, i, $j = \overline{1,n}$ be elements of the space $W_2^1(G)$ and the set of admissible domains K has the following form

$$K = \left\{D \in K_0,\ S_D \in C^2\right\} \tag{5}$$

Here K_0 is some convex subset of M_0 and it is a class of convex bounded sets $D \in R^n$. Under the conditions of settings on initial values for any $D \in K$ the solution of problem (2), (3) exists and it is reched only from $W_2^2(D)$.

Suppose, that $F(x, u, z)$ is continuous differentiable and $\frac{d}{dx}F_z(x, u, z)$ is continuous in $G \times R^n \times R^n$. Additionally, suppose, that $a_{ij}(x)$, $g(x)$ are continuous and differentiable in G.

Let $\psi = \psi(x)$ be a solution of the following problem

$$\sum_{i,j=1}^{n} (a_{ij}(x)\psi_{x_i})_{x_i} + a(x)\psi = \sum_{i=1}^{n} \left(\frac{\partial F}{\partial u_{x_i}}\right)_{x_i} - \frac{\partial F}{\partial u},\ x \in D, \tag{6}$$

$$\psi(\xi) = 0,\ \xi \in S_D, \tag{7}$$

We call this problem as adjoined problem of (1)-(3).

Let the left hand side of (6) belongs to $W_2^1(G)$. This is possible, for example, when F is linear with respect to u_x or the solution of (2), (3) is more smooth. Then for any $D \in K$ the solution of problem (6), (7) exists and is available only from $W_2^2(D)$.

Let M be a set of all convex bounded reserved sets from R^n. The operations of addition and multiplication by the non-negative number are defined in M

$$A + B = \{c = a + b : a \in A,\ b \in B\},$$

$$\lambda A = \{\lambda a : a \in A\},\ \lambda \geq 0$$

M is not linear space (the operation of subtraction is not defined in M). Let's consider the pairs (A, B), where $A, B \in M$ and define the following operations:

$$\begin{aligned} (A_1, B_1) + (A_2, B_2) &= (A_1 + A_2, B_1 + B_2), \\ \lambda(A, B) &= (\lambda A, \lambda B),\ if\ \lambda \geq 0 \\ \lambda(A, B) &= (|\lambda| B, |\lambda| A),\ if\ \lambda < 0. \end{aligned}$$

Pairs (A, B) and (C, D) are equivalent if $A + D = B + C$. The set of all such pairs is a linear space. In this space we have a scalar product: Let

$$a = (A_1, A_2), b = (B_1, B_2), A_i, B_j \in M, i = 1, 2$$

then the scalar product is defined as

$$(a, b) = \int_{S_B} P(\xi) q(\xi) d\xi$$

Here $P(x) = P_{A_1}(x) - P_{A_2}(x)$, $q(x) = P_{B_1}(x) - P_{B_2}(x)$,
$P_{A_i}(x)$, $P_{B_i}(x)$, $i = 1, 2$ are support functions of the set A_i, B_i respectively and S_B is a border of the unitt sphere B.

It may be shown that this definition satisfies all requirements of the scalar product. We define this space by $ML_2(B)$ or ML_2. If in the definition of scalar product we take any $D \in M$ instead of B, then corresponding space is defined by $ML_2(D)$.

Now we choose any class of sets from M with smooth borders.

For any $A \in M$

$$P_A(x) = \max_{l \in A} (l, x)$$

Suppose, the maximum is attained when $l = a(x) \in A$, $x \in B$. It is known, that for almost all $x \in B$ the class of sets is $a(x) \in A$. By W, we define the class of sets $D \in M$, in which $a = a(x) \in W_2^1(B)$.We take $a = (A_1, A_2), B = (B_1, B_2), A_i, B_i \in W$, $i = 1, 2$.

The scalar product (a, b) in $W \times W$ is given by

$$(a, b) \int_B \left[\Delta a(x) \Delta b(x) + \frac{\partial \Delta a(x)}{\partial x} \cdot \frac{\partial \Delta b(x)}{\partial x} \right] dx$$

Here $\Delta a(x) = a_2(x) - a_1(x)$, $\Delta b(x) = b_2(x) - b_1(x)$, $a_i(x)$, $b_i(x)$ are defined by the above given method for A_i, B_i, $i = 1, 2$. This space with the given scalar product is labeled by WL_2. If in definition of scalar product we take D instead of B, then corresponding space will be denoted by $WL_2(D)$. Note that in WL_2, the scalar product may be given as

$$(a, b) = \int_B \Delta a(x) \Delta b(x) dx.$$

Theorem 1. Let $D^* \in K$ be a solution of problem (1)-(3). Then for any $D \in K$ the following condition holds

$$\int_{S_{D^*}} [F(\xi, u^*(\xi), u_x^*(\xi)) - \sum_{i=1}^{n} \left(F_{u_{x_i}}(\xi, u^*(\xi), u_x^*(\xi)) u_{x_i}^*(\xi) - g_{x_i}(\xi) \right) -$$

$$-\sum_{i,j=1}^{n} a_{ij}(\xi)\psi^*_{x_i}(\xi)\left(u^*_{x_i}(\xi)-g_{x_i}(\xi)\right)][P_D(n(\xi))-P_{D^*}(n(\xi))]d\xi \geq 0 \qquad (8)$$

Here $u^* = u^*(x)$, $\psi^* = \psi^*(x)$ is a solution of (2),(3) and (6),(7) when $D = D^*$, respectively.

Proof. It is evident, that if $S_D \in C^2$, then $([D],0) \in WL_2$. Let us take arbitrary $D, \overline{D} \in K$, which satisfies $\|d\|_{WL_2} \leq h$, $h > 0$ is small number,

$$d = \left([D], \left[\overline{D}\right]\right), [D] = D \cup S_D, \ \overline{u} \equiv \overline{u}(x, \overline{D}), \ \Delta u = \overline{u} - u, \ D(h) \equiv \overline{D} \cap D,$$

$$\Delta D \equiv \overline{D} \backslash D(h), \ \Delta_1 \equiv \overline{D} \backslash D, \ S(h) \equiv S_{D(h)}, \ S \equiv S_D.$$

Let us write equation (2),(3) for the $\overline{D} \in K$:

$$\sum_{i,j=1}^{n} \left(a_{ij}(x)\overline{u}_{x_i}\right)_{x_j} + a(x)\overline{u} = f, \ x \in \overline{D}, \qquad (9)$$

$$\overline{u}(\xi) = g(\xi), \ \xi \in S_{\overline{D}}. \qquad (10)$$

Subtracting (2) from (9) we obtain

$$\sum_{i,j=1}^{n} \left(a_{ij}(x)\Delta u_{x_i}\right)_{x_j} + a(x)\Delta u = 0, \ x \in D(h) \qquad (11)$$

For any $\psi^{(h)} = \psi^{(h)}(x) \in W_2^2(D(h))$, we obtain from (11)

$$\begin{aligned} 0 &= \int_{D(h)} \left[\sum_{i,j=1}^{n} \left(a_{ij}(x)\Delta u_{x_i}\right)_{x_j} + a(x)\Delta u\right] \psi^{(h)} dx = \qquad (12) \\ &= \int_{D(h)} \left[\sum_{i,j=1}^{n} \left(a_{ij}(x)\psi^{(h)}_{x_i}\right)_{x_j} + a(x)\psi^{(h)}\right] \Delta u dx + \\ &\quad + \int_{S(h)} \frac{\partial \Delta u}{\partial N}\psi^{(h)}(\xi)d\xi - \int_{S(h)} \Delta u(\xi)\frac{\partial \psi^{(h)}}{\partial N}d\xi, \end{aligned}$$

where $\frac{\partial \Delta u}{\partial N} = \sum_{i,j=1}^{n} a_{ij}(x)\Delta u_{x_i}\cos(n, x_j)$, n ,is unit normal to $S(h)$.

Calculate the increment of the functional (1)

$$\Delta I = I(\bar{D}) - I(D) = \int_{\bar{D}} F(x, \bar{u}(x), \bar{u}_x(x))dx - \int_{D} F(x, u(x), u_x(x))dx =$$

$$= \int_{D(h)} \left[F(x, \bar{u}(x), \bar{u}_x(x)) - F(x, u(x), u_x(x))\right] dx +$$

$$+ \int_{\Delta D} F(x, \bar{u}(x), \bar{u}_x(x))dx - \int_{\Delta D} F(x, u(x), u_x(x))dx.$$

Substituting the right hand side of the relation (12) here (so the left hand side of this relation is equal to zero) we obtain

$$\Delta I = \int\limits_{D(h)} \Big[F_u(x,u,u_x) - \sum_{i=1}^{n} \frac{d}{dx_i} F_{u_{x_i}}(x,u,u_x) + \\ + \sum_{i,j=1}^{n} (a_{ij}(x)\psi^{(h)}_{x_i})_{x_j} + a(x)\psi^{(h)} \Big] \Delta u dx + \tag{13}$$

$$+ \sum_{i=1}^{n} \int\limits_{D(h)} \frac{d}{dx}(F_{u_x}(x,u(x),u_x(x))\Delta u(x)dx + \int\limits_{\Delta\bar{D}} F(x,\bar{u},\bar{u}_x)dx -$$

$$- \int\limits_{\Delta D} F(x,u,u_x)dx + \int\limits_{S(h)} \frac{\partial \Delta u}{\partial N}\psi^{(h)}d\xi - \int\limits_{S(h)} \Delta u \frac{\partial \psi^{(h)}}{\partial N}d\xi + o(\|\Delta u\|_{W_2^1})$$

Let $\psi^{(h)} = \psi^{(h)}(x)$ be a solution of the following problem

$$\sum_{i,j=1}^{n} (a_{ij}\psi^{(h)}_{x_i})_{x_j} + a\psi^{(h)} = \sum_{i=1}^{n} \frac{d}{dx_i} F_{u_{x_i}} - F_u, x \in D(h) \tag{14}$$

$$\psi^{(h)}(\xi) = 0, \xi \in S(h) \tag{15}$$

We call this problem quasiadjoint problem of (1)-(3). Considering it in (13) we obtain

$$\Delta I = I_1 + I_2 + I_3 + o(\|\Delta u\|_{W_2^1(D(h))}), \tag{16}$$

where

$$I_1 = \int\limits_{\Delta\bar{D}} F(x,\bar{u}(x),\bar{u}_x(x))dx,\ I_2 = -\int\limits_{\Delta D} F(x,u(x),u_x(x))dx,$$

$$I_3 = \sum_{i=1}^{n} \int\limits_{D(h)} \frac{d}{dx_i}(F_{u_{x_i}}(x,u(x),u_x(x))\Delta u(x)dx - \int\limits_{S(h)} \Delta u(\xi)\frac{\partial \psi^{(h)}}{\partial N}d\xi$$

We transfer each of $I_i, i = \overline{1,3}$ in the following way

$$I_1 = \int\limits_{\Delta\bar{D}} F(x, \bar{u}(x), \bar{u}_x(x))dx = \int\limits_{\bar{D}} F(x, \bar{u}(x), \bar{u}_x(x))dx -$$

$$- \int\limits_{D(h)} F(x, \bar{u}(x), \bar{u}_x(x))dx =$$

$$= \int\limits_{S(h)} F(\xi, \bar{u}(\xi), \bar{u}_x(\xi)) \left[P_{\bar{D}}(n(\xi)) - P_{D(h)}(n(\xi))\right] d\xi + O(h) = \tag{17}$$

$$= \int\limits_{S(h)} F(\xi, u(\xi), u_x(\xi)) \left[P_{\bar{D}}(n(\xi)) - P_{D(h)}(n(\xi))\right] d\xi + o(\|\Delta u\|_{W_2^1(D(h))}) + o(h)$$

Similarly

$$I_2 = - \int\limits_{\Delta D} F(x, u(x), u_x(x))dx = \int\limits_{D(h)} F(x, u(x), u_x(x))dx -$$

$$- \int\limits_{D} F(x, u(x), u_x(x))dx = - \int\limits_{S(h)} F(\xi, u(\xi), u_x(\xi)) \left[P_D(n(\xi)) - \right. \tag{18}$$

$$\left. P_{D(h)}(n(\xi))\right] d\xi + o(h).$$

Adding (17) and (18) we obtain

$$I_1 + I_2 = \int\limits_{S(h)} F(\xi, u(\xi), u_x(\xi)) \left[P_{\bar{D}}(n(\xi)) - P_D(n(\xi))\right] d\xi + \tag{19}$$

$$+ O(\|\Delta u\|_{W_2^1(D(h))}) + O(h)$$

Now we transfer I_3

$$I_3 = \sum_{i=1}^{n} \int\limits_{D(h)} \frac{d}{dx_i}(F_{u_{x_i}}(x, u(x), u_x(x))\Delta u(x))dx -$$

$$- \sum_{i,j=1}^{n} \int\limits_{D(h)} \frac{d}{dx_i}((a_{ij}(x)\frac{\partial \psi^{(h)}}{\partial x_j})\Delta u(x))dx =$$

$$= \sum_{i,j=1}^{n} \int\limits_{D(h)} \frac{d}{dx_i}(F_{u_{x_i}}(x, u(x), u_x(x)) - a_{ij}(x)\frac{\partial \psi^{(h)}}{\partial x_j})\Delta u(x)dx +$$

$$+\sum_{i,j=1}^{n}\int\limits_{D(h)}(F_{u_{x_i}}(x,u(x))-a_{ij}(x)\frac{\partial\psi^{(h)}}{\partial x_j})\Delta u_{x_i}(x)dx.$$

Considering that $\psi^{(h)}=\psi^{(h)}(x)$ is a solution of problem (14) , (15), we obtain

$$I_3=\int\limits_{D(h)}F_u(x,u(x),u_x(x))\Delta u(x)dx+$$

$$+\sum_{i=1}^{n}\int\limits_{D(h)}(F_{u_{x_i}}(x,u(x),u_x(x))-\sum_{j=1}^{n}a_{ij}(x)\frac{\partial\psi^{(h)}}{\partial x_j})\Delta u_{x_i}(x)dx.$$

We considered the boundary conditions (3) and (10). Then considering, that $u(\xi)=g(\xi),\xi\in S(D)$, we have

$$I_3=-\int\limits_{S(h)}\left[\sum_{i=1}^{n}(F_{u_{x_i}}(\xi,u(\xi),u_x(\xi))-\sum_{j=1}^{n}a_{ij}(\xi)\frac{\partial\psi}{\partial x_j}\right]\times$$

$$\times\left[u_{x_i}(\xi)-g_{x_i}(\xi)\right]\left[P_{\bar{D}}(n(\xi))-P_D(n(\xi))\right]d\xi+$$

$$+o(h)+o(\|\Delta u\|_{W_2^1(S(h))}) \tag{20}$$

Adding (19) and (20) to (16) we get

$$\Delta I=\int\limits_{S(h)}\left[F(\xi,u(\xi),u_x(\xi))-\sum_{i=1}^{n}(F_{u_{x_i}}(\xi,u(\xi),u_x(\xi))-\sum_{j=1}^{n}a_{ij}(\xi)\psi(x))\right]\times$$

$$\times\left[u_{x_i}(\xi)-g_{x_i}(\xi)\right]\left[P_{\bar{D}}(n(\xi))-P_D(n(\xi))\right]+$$

$$+o(h)+o(\|\Delta u\|_{W_2^1(D(h))})+o(\|\psi\|_{W_2^1(D(h))}). \tag{21}$$

If we show that $r(h)\equiv o(\|\Delta u\|_{W_2^1(D(h))})+o(\|\Delta\psi\|_{W_2^1(D(h))})=o(h)$, then from (21) we obtain the following for expressing the first variation

$$\delta I(D,\bar{D})=\int\left[F(\xi,u(\xi),u_x(\xi))+\sum_{i,j=1}^{n}(a_{ij}(\xi))\psi_{x_j}-F_{u_{x_i}}(\xi,u(\xi),u_x(\xi))\times\right.$$

$$\left.\times(u_{x_i}(\xi)-g_{x_i}(\xi))\left[P_{\bar{D}}(n(\xi))-P_D(n(\xi))\right]d\xi.\right. \tag{22}$$

Here considering that $D^* \in K$ is a solution of problem (1)-(3) we obtain (8). Therefore , in order to complete the proof it is sufficient to show that

$$\|\Delta u\|_{W_2^1(D(h))} + \|\Delta u\|_{W_2^1(d(h))} \leq Lh \ , \tag{23}$$

where $h > 0$ is constant. At first, we estimate $\|\Delta u\|_{W_2^1(D(h))}$. Considering boundary conditions (3),(10) we have

$$\Delta u(\xi_h) = \bar{u}(\xi_h) - u(\xi_h) = \begin{cases} \bar{u}(\bar{\xi}) - u(\bar{\xi}), & if \ \ \xi_h \in \bar{S}, \\ \bar{u}(\xi) - u(\xi) & if \ \ \xi \in S \end{cases} =$$

$$= \begin{cases} u(\xi) - u(\bar{\xi}), & if \ \ \xi_h \in \bar{S}, \\ \bar{u}(\xi) - \bar{u}(\bar{\xi}) & if \ \ \xi_h \in S \end{cases} = \begin{cases} (u_x(\xi), \xi - \bar{\xi}), & if \ \ \xi_h \in \bar{S}, \\ (\bar{u}_x(\xi), \xi - \bar{\xi}) & if \ \ \xi_h \in S. \end{cases}$$

Taking into account that $d = ([D], \left[\bar{D}\right]) \in WL_2, \|d\|_{WL_2} \leq h, \|u\|_{W_2^1(s)} \leq const, \|\bar{u}\|_{W_2^1(S)} \leq const$ we obtain from the last expression

$$\|\Delta u\|_{L_2(S(h))} \leq L_1 \cdot h,$$

where L_1 is any positive number. So $\Delta u = \Delta u(x)$ satisfies condition (11) and we have

$$I_3 = \sum_{i=1}^{n} \int\limits_{D(h)} \left[F_u(.)\Delta u(x) + \sum_{i=1}^{n} \left(F_{u_{x_i}}(.) - \sum_{j=1}^{n} a_{ij}(x) \frac{\partial \psi^{(h)}}{\partial x_j} \right) \Delta u_{x_i}(x) \right] dx +$$

$$+ \sum_{i=1}^{n} \int\limits_{D} \left(F_{u_{x_i}}(.)(u(x) - g(x)) + \sum_{j=1}^{n} \frac{d}{dx_i} (a_{ij}(x)(u(x) - g(x)) \frac{\partial \psi^{(h)}}{\partial x_j} \right) dx -$$

$$- \sum_{i=1}^{n} \int\limits_{\bar{D}} \left(\frac{d}{dx_i} F_{u_{x_i}}(.)(\bar{u}(x) - g(x)) + \sum_{j=1}^{n} \frac{d}{dx_i} (a_{ij}(x)(\bar{u}(x) - g(x)) \frac{\partial \psi^{(h)}}{\partial x_j} \right) dx.$$

It is supposed that $\psi(x) = 0$ outside of the D. Then we have

$$I_3 = \int\limits_{D(h)} \left[F_u(.)\Delta u + \sum_{i=1}^{n} \left(F_{u_{x_i}}(.) - \sum_{j=1}^{n} a_{ij}(x) \frac{\partial \psi}{\partial x_j} \right) \Delta u_{x_i} \right] dx +$$

$$+ \int\limits_{D} \left[F_u(.)(u(x) - g(x)) + \sum_{j=1}^{n} \left(F_{u_{x_i}}(.) - \sum_{j=1}^{n} a_{ij}(x) \frac{\partial \psi}{\partial x_j} \right) (u_{x_i}(x) - g_{x_i}(x)) \right] dx +$$

$$+\int_{\bar{D}}\left[F_u(.)(\bar{u}(x)-g(x))+\sum_{i=1}^{n}\left(F_{u_{x_i}}(.)-\sum_{j=1}^{n}a_{ij}(x)\frac{\partial\psi}{\partial x_j}(\bar{u}_{x_i}(x)-g_{x_i}(x))\right)dx\right]+$$

$$+o(\left\|\psi^{(h)}-\psi\right\|_{W_2^1(D(h))})).$$

For simplicity we omitted here the arguments of F. Similar to the calculation of I_2, we obtain

$$I_3=-\int_{S(h)}\left[F_u(.)u+\sum_{i=1}^{n}\left(F_{u_{x_i}}-\sum_{j=1}^{n}a_{ij}\frac{\partial\psi}{\partial x_j}\right)u_{x_i}\right].[P_{\bar{D}}(n(\xi))-P_D(n(\xi))]\,d\xi+$$

$$+\int_{S(h)}\left[F_u(.)g(\xi)+\sum_{i=1}^{n}\left(F_{u_{x_i}}(.)-\sum_{j=1}^{n}a_{ij}(\xi)\frac{\partial\psi}{\partial x_j}\right)g_{x_i}(\xi)\right].[P_{\bar{D}}(n(\xi))-P_D(n(\xi))]\,d\xi+$$

$$+O(h)+o(\|\Delta u\|_{W_2^1(D(h))})+o(\|\Delta\psi\|_{W_2^1(D(h))}).$$

Where $\Delta\psi=\psi^{(h)}(x)-\psi(x)$

From these relations we can obtain that

$$I_3=\int_{S(h)}[F_u(\xi,u(\xi),u_x(\xi))(u(\xi)-g(\xi))+$$

$$+(\sum_{i=1}^{n}F_{u_{x_i}}(\xi,u(\xi),u_x(\xi))-\sum_{j=1}^{n}a_{ij}(\xi)\frac{\partial\psi}{\partial x_j}(u_{x_j}(\xi)-g_{x_i}(\xi))\times$$

$$\times[P_{\bar{D}}(n(\xi))-P_D(n(\xi))]\,d\xi+o(h)+o(\|\Delta u\|_{W_2^1(D(h))})+o(\|\Delta\psi\|_{W_2^1(D(h))})$$

$$\|\Delta u\|_{W(D(h))}\le L_2\cdot h\ ,\ L_2>0.$$

We can show similarly that

$$\|\Delta\psi\|_{W_2^1(D(h))}\le L_3h.$$

The proof is finished.

Lemma. Let D_0 be any convex bounded domain and $A(x)$ is continuous in D_0. If the condition

$$\int_{S_{D_0}}A(\xi)\left[P_D(n(\xi))-P_{D_0}(n(\xi))\right]d\xi\ge 0$$

holds for arbitrary $D\in M$, then $A(\xi)=0$ in S_{D_0}.

Proof. Let's take any $H \in M, D = D_0 + H$

$$P_{[D]}(x) = P_{[D_0]}(x) + P_{[H]}(x).$$

Considering it in (21); we have

$$\int_{S_{D_0}} A(\xi) P_H(n(\xi)) d\xi \geq 0 \tag{24}$$

D_0 is convex domain, and there exist such a domain $\overline{D}$ and a number $\varepsilon > 0$, that $D_0 = \overline{D} + \varepsilon H$. Taking $D = \overline{D}$ in (21) and considering that $P_{D_0}(x) = P_{\overline{D}}(x) + \varepsilon P_H$ we have

$$\int_{S_{D_0}} A(\xi) P_H(n(\xi)) d\xi \leq 0.$$

Considering (23), we obtain

$$\int_{S_{D_0}} A(\xi) P_H(n(\xi)) d\xi = 0, \ \forall H \in M_0.$$

It is known that every positive homogeneous continuous function $h(x)$ may be presented in the following form [6]

$$h(x) = \lim_{n\to\infty} \left[P_{H_1^{(n)}}(x) - P_{H_2^{(n)}}(x)\right],$$

where $H_1^{(n)}, H_2^{(n)} \in M_0$, $n = 1, 2, ...$

Then, for every positive homogeneous function $h(x)$ it holds that

$$\int_{S_{D_0}} A(\xi) h(\xi) d\xi = 0.$$

Where, from last equality, we have

$$A(\xi) = 0.$$

The lemma is proved.

From Theorem 1 and Lemma 1 we can state the following theorem.

Theorem 2. Let $D^* \in K$ be a solution of problem (1)-(3) and $K_0 = M_0$, then it is true that

$$F(\xi, u^*(\xi), u_x^*(\xi)) + \sum_{i,j=1}^{n} a_{ij}(\xi) \psi_{x_j}^*(\xi) \left(u_{x_i}^*(\xi) - g_{x_i}(\xi)\right) -$$

$$-\sum_{i=1}^{n} F_{u_{x_i}}\left(\xi, u^*(\xi), u_x^*(\xi)\right)\left(u_{x_i}^*(\xi) - g_{x_i}(\xi)\right), \xi \in S_{D^*}. \tag{25}$$

Note 1. Let K be a class of two connected domains $D \in R^n$, with $D_0 \in R^n$, where $D = D_1 \backslash D_0$, $D_0, D_1 \in M_0$.

Then, writing

$$\int_D f(x)\,dx = \int_{D_1} f(x)\,dx - \int_{D_0} f(x)\,dx$$

we similarly can prove the next condition

$$\sum_{k=1}^{1}(-1)^{k+1}\int_{S_{D_k^*}}\left[F\left(\xi, u^*(\xi), u_x^*(\xi)\right)\right] + \sum_{i,j=1}^{n} a_{ij}(\xi)\,\psi_{x_j}^*(\xi)\left(u_{x_i}^*(\xi) - g_{x_i}(\xi)\right) -$$

$$-\sum_{i=1}^{n} F_{u_{x_i}}\left(\xi, u^*(\xi), u_x^*(\xi)\right)\left(u_{x_i}^*(\xi) - g_{x_i}(\xi)\right) \times$$

$$\times\left[P_{\overline{D}_k}\left(n(\xi)\right) - P_{D_k}\left(n(\xi)\right)\right] d\xi \geq 0 \tag{26}$$

In this case the conditions (24) and (25) will not change.

Similar to the conditional gradient method, we find the numerical solution of this problem using the expression of the first variation.

Step 1. We take the initial domain $D^{(0)} \in K$ and solving problem (2),(3) find $u^0 = u^0(x)$.

Step 2. Knowing $D^{(0)}$ and $u^0 = u^0(x)$, problem (6), (7) is solved and $\psi^0 = \psi^0(x)$ is defined.

Step 3. Calculating

$$A^{(0)}(\xi) = F(\cdot) - \sum_{i,j=1}^{n} a_{ij}\psi_{x_j}^{(0)}\left(u_{x_i}^{(0)} - g_{x_i}\right)_{x=\xi}$$

we solve the problem

$$I_0(p) = \int_{S_{D^{(0)}}} A^0(\xi)\,P\left(n(\xi)\right)d\xi \to \min$$

This problem is solved on the set K. If for example K_0 has the from of

$$K_0 = \{D \in R^n, D_0 \subset D \subset D_1\},$$

$I_0(p)$ is minimized under the condition of

$$P_{D_0}(x) \leq p(x) \leq P_{D_1}(x),\ x \in R^n.$$

Step 4. Using the formula $\overline{D}^{(0)} = \partial P^{(0)}(0)$, where $\partial P^{(0)}(0)$ is subdifferential of the function $P^{(0)}(x)$ at the point $0 \in R^n$ the auxiliary domain is defined. Next domain is defined in the form of

$$D^{(1)} = (1-\alpha) D^{(0)} + \alpha \overline{D}^{(0)}, \ 0 < \alpha < 1.$$

Here α is chosen by several methods [5]. This process is continued untill we reach any exactness condition.

References

[1] Banichuk N. V. (1975). Optimization of elastic bars in torsion.-*Rept. Dan. Gent. Appl. Math. and Mech.*, No.86.

[2] Banichuk N. V. (1980). *The optimization of the elastic bodies.*-M.

[3] Kerimov A. K. (1982). On a problem with free borders.-*DAN SSSR*, Vol.266, No.3.

[4] Ladizhenskaya O. A. (1973). *The boundary problems of mathematical physics.*-M.

[5] Vasilyev F. P. (1981). *The method of solution of extremal problems.*-M.

[6] Demyanov V. F. Rubinov A. M. (1990). *The bases on non-smooth analyses and quasidifferential calculus.*-M.

ÖZET

Bir çok pratik problemler, özellikle esneklik, hidrodinamik, jeofizik ve istatistiksel kontrol uygulamaları, aerodinamic teorilerinin problemleri optimal formların bulunması koşullarını ortaya çıkartmaktadır. Bu problemlerin çok güncel ve önemli olmasına rağmen çözümlerinde bir çok matematiksel zorluklar ortaya çıkmaktadır. Bu makalede elliptik denklem içeren optimal kontrol problemlerinin çözümleri için genel bir yöntem önerilmektedir. Bu yöntem yukarıda adı geçen problemler genelinde bir yaklaşım ve onların çozümleri için etkin sayısal algoritmalar kurmaya imkan vermektedir.

İstatistik, Journal of the Turkish Statistical Association
1999, Vol.2, No 3, pp. 187-192

GEOMETRIC INTERPRETATION OF PRIME POWER LATTICE DESIGNS

Soner Gönen and Hülya Bayrak
Gazi University, Faculty of Arts & Sciences, Department of Statistics
Teknikokullar, Beşevler, Ankara, Turkey

Abstract

In this study, the geometric representation of Balanced Prime-Power Lattice Design is obtained by finite analytic projective geometry of Galois Field GF(pn) of m-dimensions, which can be denoted by PG(m, pn) and finite Euclidean Geometry. Definition of homogeneous replications is given by the properties of PG(m, pn). Furthermore, a geometric way of obtaining homogeneous replications is also given.

Key Words: Prime-power Lattice design, finite analytic projective geometry.

1. Introduction

In an experiment that includes a lot of varieties, placing these varieties into the blocks is very difficult, sometimes it is impossible. The variance between the blocks is less than the variance within the blocks in some placements. This is not the desired situation. In this case, Lattice design looks like the factorial design where each variety is considered as a single factor or a combination of factors. This experiment is called as *Quasi Factorial Design*, *Lattice Design* or it can be called *Prime-Power Lattice Design*. This type of experiment is used when obtaining the homogeneous data is difficult. These designs have been used first by Yates in 1936.

The effects of some prime-power factors and the effects of interactions of these factors are mixed with the effects of blocks in various repetitions. As a result, decreases are observed in the variance within the blocks in comparison with the variance between the blocks and effectiveness is obtained in the tests of non-mixed factors and interactions in comparison with the randomized block design.

The p^n varieties and treatment combinations can be represented by an n-dimensional Lattice, each side of which have p points where p is a prime number. We will place these p^n varieties into the blocks of size p in randomized order. Since p^n denotes the power of a prime number, the design which we are interested in is called ***Balanced Prime-Power Lattice Design***.

In this paper, number of blocks is denoted by b, number of treatments or treatment combinations is denoted by t, block size is denoted by k, number of replications of treatments

or treatment combinations is denoted by r and the number of varieties is p^n. Number of replications of each pair of the treatments or treatment combinations is denoted by λ. p is the level of pseudo factors. So, in accordance with these notations the Balanced Prime-Power Lattice Design has the following properties:

$$\lambda = \frac{r(k-1)}{t-1} \quad (1)$$

$$r = p+1 \quad (2)$$

$$bk = rt \quad (3)$$

The cases where the number of varieties is a prime number or power of a prime number have been given first in [2], [3] and [4] but the geometric interpretations have not been given in these studies.

2. Geometric Meaning of Balanced Prime-Power Lattice Design

p^n varieties has p^n-1 degrees of freedom. To test any of the pseudo factors or pseudo factor combinations, we have p groups each of that has p^{n-1} varieties and p-1 degrees of freedom. p^n-1 can be called total degrees of freedom and p-1 can be called degrees of freedom of groups. We can form $p^{n-1}+p^{n-2}+...+p+1$ different treatment or treatment combination groups, which are the number of blocks of Balanced Prime-Power Lattice Design and the number of treatments or treatment combinations of Balanced Prime-Power Lattice Design, by dividing the total degrees of freedom p^n-1 by the degrees of freedom of groups p-1.

Furthermore, a one-by-one relationship can be formed between the Balanced Prime-Power Lattice Design and the Galois Field $GF(p^n)$. Assume that the projective geometry constructed on $GF(p^n)$ is $PG(m, p^n)$. We assumed in this study that the varieties of the Balanced Prime-Power Lattice Design are the points and the blocks of the Balanced Prime-Power Lattice Design are the lines of $PG(m, p^n)$.

If we delete any line of $PG(m, p^n)$ with the points on it, we obtain finite Euclidean Geometry $EG(m, p^n)$ constructed on $GF(p^n)$. The idea of deleting a line can be considered as grouping p^n varieties according to treatments or treatment combinations which are the points of the deleted line.

There are $p+1$ lines at each point of $PG(m, p^n)$. Because of the Lattice design, there are also $p+1$ points on each line of $PG(m, p^n)$. After deleting a line, there are p points on each line of $EG(m, p^n)$. Every point of the deleted line was a common point of $p+1$ different lines of $PG(m, p^n)$. Remaining p^2 lines of $EG(m, p^n)$, after deleting a line of $PG(m, p^n)$, are non-crossing lines which constitute $p+1$ groups. These $p+1$ groups are called homogeneous replications and these homogeneous replications allow us to compare all treatments or treatment combinations. So, it is important. Let us explain these things said up to now with an example.

Example:

For the purpose of illustration, designs for $27=3^3$ varieties, where $p=3$ and $n=3$, will be considered. There are $p^2+p+1=13$ lines in $PG(2, 3)$. Since the design is balanced there are also $p^2+p+1=13$ points.

In this Balanced Prime-Power Lattice Design the number of treatments is $t=3$, number of replications of treatments is $r=4$, block size is $k=4$, number of replications of each pair of the treatments is $\lambda=1$ and there are 13 blocks. These 13 lines and points as we wrote above can be shown as in *Table-1* below:

Table-1 Lines and Points of PG(2, 3)

Line Number	Lines	A	B	AB	AB^2	C	AC	AC^2	BC	BC^2	ABC	ABC^2	AB^2C	AB^2C^2	u	h
1	[0,0,1]	X	X	X	X										7	27
2	[0,1,0]	X				X	X	X							7	27
3	[0,-1,1]	X							X		X			X	11	23
4	[0,1,1]	X								X		X	X		12	22
5	[1,0,0]		X			X			X	X					7	27
6	[1,0,-1]		X				X				X		X		10	24
7	[1,0,1]		X					X				X		X	13	21
8	[1,-1,0]			X		X					X	X			10	24
9	[-1,1,1]			X				X	X				X		11	23
10	[1,-1,1]				X	X							X	X	13	21
11	[1,1,0]			X			X			X				X	12	22
12	[1,1,-1]				X		X		X			X			11	23
13	[1,1,1]				X			X		X	X				12	22

In this table, u is the total of the powers of letters in the related row and h is the number computed by

(4) $$h = \frac{136 - ru}{k}$$

The representation of Table-1 above is given by *Figure-1* below:

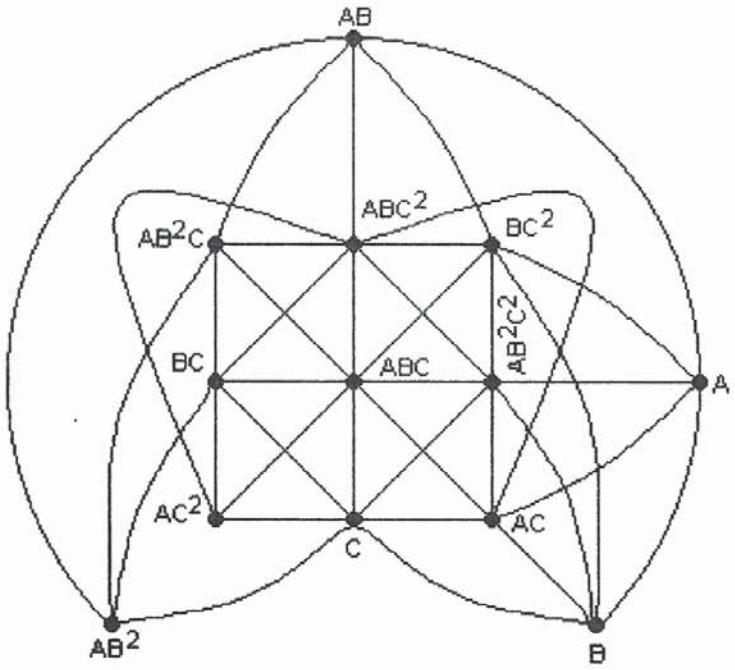

Figure-1 Representation of Table-1 in PG(2, 3)

The lines and points on that lines in *PG(2, 3)* are as follows:

Table-2 Lines and Points in PG(2, 3)

LINES	POINTS			
[0, 0, 1]	(1, 1, 0)	(1, 0, 0)	(0, 1, 0)	(1, -1, 0)
[0, 1, 0]	(1, 0, 1)	(1, 0, 0)	(0, 0, 1)	(1, 0, -1)
[0, -1, 1]	(1, 1, 1)	(0, 1, 1)	(1, 0, 0)	(-1, 1, 1)
[0, 1, 1]	(1, 0, 0)	(0, -1, 1)	(1, -1, 1)	(1, 1, -1)
[1, 0, 0]	(0, 1, 0)	(0, 1, 1)	(0, 0, 1)	(0, -1, 1)
[1, 0, -1]	(1, 0, 1)	(1, 1, 1)	(1, -1, 1)	(0, 1, 0)
[1, 0, 1]	(0, 1, 0)	(1, 0 , -1)	(-1, 1, 1)	(1, 1, -1)
[1, -1, 0]	(1, 1, 1)	(0, 0, 1)	(1, 1, 0)	(1, 1, -1)
[-1, 1, 1]	(1, 1, 0)	(1, 0, 1)	(-1, 1, 1)	(0, -1, 1)
[1, -1, 1]	(1, 1, 0)	(0, 1, 1)	(1, 0, -1)	(1, -1, 1)
[1, 1, 0]	(0, 0, 1)	(1, -1, 1)	(-1, 1, 1)	(1, -1, 0)
[1, 1, -1]	(0, 1, 1)	(1, 0, -1)	(1, -1, 0)	(1, 1, -1)
[1, 1, 1]	(1, 1, 1)	(1, -1, 0)	(1, 0, -1)	(0, -1, 1)

Since the treatment combinations AB and AC are mixed, the combinations BC^2 and AB^2C^2 are also mixed. As a result, the 11^{th} line of Table-1 that includes these 4 treatment combinations is chosen as a mixed system and this 11^{th} line is removed from *PG(2, 3)* because of mixing combinations. So, we reach to *EG(2, 3)* from *PG(2, 3)*. *EG(2, 3)* consists of $p^2+p=12$ lines and $p^2=9$ points because the mixed line with points is removed.

To obtain homogeneous replications, any point of 11^{th} line will be deleted. For example, we delete the point $AB^2C^2=(1, -1, -1)$. So, 4 lines of *PG(2, 3)* (or 3 lines of *EG(2, 3)*) of Figure-1 which pass through $AB^2C^2=(1, -1, -1)$ become the lines with no common points (they become parallel lines in some sense). Since 11^{th} line is removed, we have 3 lines in *EG(2, 3)* which correspond to the group of *Homogeneous Replications-1* as follows:

Table-3 Homogeneous Replication-1

Line Number	Homogeneous Replication-1	Deleted Point
3	A, BC, ABC	AB^2C^2
7	B, AC^2, ABC^2	AB^2C^2
10	C, AB^2, AB^2C	AB^2C^2

We can constitute 4 other homogeneous replications by deleting the points AB, AC, BC^2 of the mixed line as follows:

Table-4 Homogeneous Replication-2

Line Number	Homogeneous Replication-2	Deleted Point
1	A, B, AB^2	AB
8	C, ABC, ABC^2	AB
9	AC^2, BC, AB^2C	AB

Table-5 Homogeneous Replication-3

Line Number	Homogeneous Replication-3	Deleted Point
2	A, C, AC^2	AC
6	B, ABC, AB^2C	AC
12	AB^2, BC, ABC^2	AC

Table-6 Homogeneous Replication-4

Line Number	Homogeneous Replication-4	Deleted Point
4	A, ABC^2, AB^2C	BC^2
5	B, C, BC	BC^2
13	AB^2, AC^2, ABC	BC^2

A representation of homogeneous replications in *EG(2, 3)* is given below:

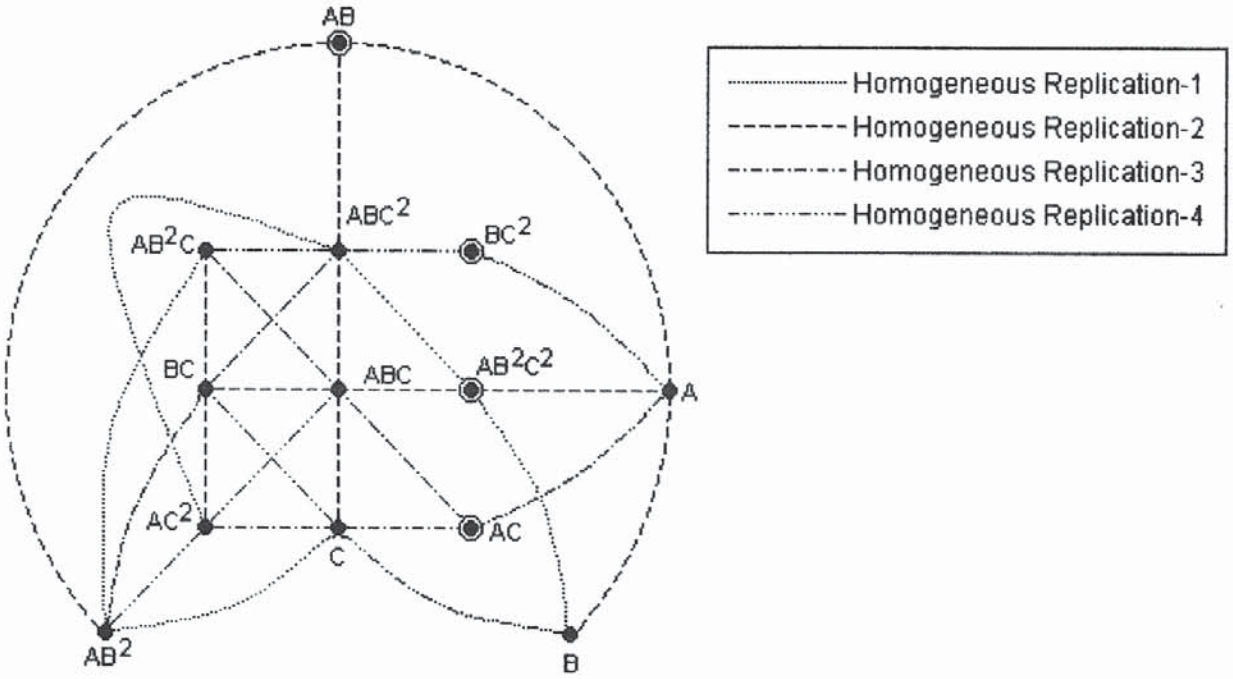

Figure-2 Representation of Four Homogeneous Replications in EG(2, 3)

Let us consider the first mixed system or mixed line of Table-1. This line includes the treatments or treatment combinations $A=(1, 0, 0)$, $B=(0, 1, 0)$, $AB=(1, 1, 0)$ and $AB^2=(1, 2, 0)$ or $AB^2=(1, -1, 0)$. The line including the 4 points above can be shown as $[0, 0, 1]$ according to the rule that points being on a line. 13 lines and 13 points make a *PG(2, 3)*.

Dual of above *PG(2, 3)* is another *PG(2, 3)* where the points of first *PG(2, 3)* are the lines of second *PG(2, 3)* and the lines of first *PG(2, 3)* are the points of second *PG(2, 3)*. Dual of points $(1, 0, 0)$, $(0, 1, 0)$, $(1, 1, 0)$ and $(1, -1, 0)$ is the line $[0, 0, 1]$ and the dual of the line $[0, 1, 1]$ is the point $C=(0, 0, 1)$ which is the common (intersection) point of the 4 points $(1, 0, 0)$, $(0, 1, 0)$, $(1, 1, 0)$ and $(1, -1, 0)$ which are the 4 lines $[1, 0, 0]$, $[0, 1, 0]$, $[1, 1, 0]$ and $[1, -1, 0]$.

First line $[1, 0, 0]$ includes 4 points that are $B=(0, 1, 0)$, $C=(0, 0, 1)$, $BC=(0, 1, 1)$ and $BC^2=(0, 1, -1)$.

Second line $[0, 1, 0]$ includes 4 points that are $A=(1, 0, 0)$, $C=(0, 0, 1)$, $AC=(1, 0, 1)$ and $AC^2=(1, 0, -1)$.

Third line *[1, 1, 0]* includes 4 points that are $C=(0, 0, 1)$, $AB^2=(1, -1, 0)$, $AB^2C=(1, -1, 1)$ and $AB^2C^2=(1, -1, -1)$.

Fourth line *[1, -1, 0]* includes 4 points which are $C=(0, 0, 1)$, $AB=(1, 1, 0)$, $ABC=(1, 1, 1)$ and $ABC^2=(1, 1, -1)$.

So, the set of points on line *[0, 0, 1]* is the dual of pencil of lines through a point *(0, 0, 1)*. As a result, the above 4 lines makes a homogeneous replication if we drop point $C=(0, 0, 1)$ from each line. Homogeneous replications allow us to test treatments or treatment combinations easily.

Similarly, we can obtain $p+1=4$ homogeneous replications for each mixed line. Since we have 13 mixed lines, we have 13 homogeneous replication groups each having 4 homogeneous replications.

Geometrically, the 3 lines of each homogeneous replication are independent (non-crossing). As a result, levels of remaining 9 treatments (points) or treatment combinations can be compared which implies that the remaining treatments or treatment combinations can be tested easily.

References

[1] Kempthorne, O. (1952) *The Design and Analysis of Experiments.* John Wiley and Sons Inc., New York.

[2] Kempthorne, O. and Federer, W. T. (1948)The General Theory of Prime-Power Lattice Designs I; Introduction and Designs for p^n Varieties in Blocks of p Plots. *Biometrics* 4, 54-79.

[3] Kempthorne, O. and Federer, W. T. (1948) The General Theory of Prime-Power Lattice Designs II; Designs for p^n Varieties in Blocks of p^s Plots and in Squares, *Biometrics* 4, 109-121.

[4] Federer, W. T. (1949) The General Theory of Prime-Power Lattice Designs III; The Analysis for p^3 Varieties in Blocks of p Plots with More than 3 Replicates. *Biometrics*, 144-161.

ÖZET

Bu çalışmada, Balanced Prime Power Lattice Dizayn' ların geometrik yapıları sonlu cisim $GF(p^n)$ üzerine kurulan m-boyutlu projektif geometri $PG(m, p^n)$ ve Öklit geometri $GF(m, p^n)$' den faydalanılarak verildi. Homojen replikasyonların tanımı $PG(m, p^n)$' nin özellikleri kullanılarak verildi. Ayrıca, homojen replikasyonları elde etmenin geometrik bir yolu da gösterildi.

İstatistik, Journal of the Turkish Statistical Association
1999, Vol.2, No 3, pp. 193-206

FADING KALMAN FILTER FOR MANOEUVRING TARGET TRACKING

Murat Efe*
Electronics Engg. Dept.
Ankara University
Faculty of Science
Ankara, Turkey
Email:efe@science.ankara.edu.tr

Levent Ozbek
Department of Statistics
Ankara University
Faculty of Science
Ankara, Turkey
Email:ozbek@science.ankara.edu.tr

1 Abstract

In this paper a novel approach to adaptive Kalman filtering is presented. The filter utilizes a forgetting factor, which tries to adjust the state error covariance according to the changed target dynamics. The filter aims to utilize the available data in order to provide a better covarage throughout the whole target motion. The performance of the algorithm is compared with that of an interacting multiple model (IMM) algorithm and also with that of a standard Kalman filter. The proposed filter does not rely on a priori knowledge about the target motion and it produces better estimates than the IMM algorithm during manoeuvring periods.

2 Introduction

The performance of a tracking algorithm is mainly governed by the performance of the state estimator used. The Kalman filter is the traditional and the most widely used state

*The author is currently with the Institut d'Autamatique of Swiss Federal Technical Institute in Lausanne, Switzerland

estimator in target tracking applications. The filter is the general solution to the recursive linear minimum mean square estimation problem. It will minimize the mean square error between the estimates and the actual target dynamics as long as the target dynamics are accurately modelled.

The process of state estimation in the Kalman filter comprises two parallel cycles, namely, *i*) estimation of the state and *ii*) estimation of the state covariance, Fig 1. The final estimation of the state is found from the predicted state, innovation and Kalman gain. The Kalman gain is the 'ratio' of the state covariance to the innovation covariance and can be considered as a correction factor on the final estimate. From a frequency domain viewpoint the magnitude of the Kalman gain determines the bandwidth and response speed of the filter. A small gain value produces a substantial noise reduction when the target is not manoeuvring and a large gain value gives a fast response to changes in the target's dynamics, providing the filter with a larger bandwidth to cover manoeuvres. Basically, it can be said that the performance of the Kalman filter is determined by the size of the Kalman gain. While the Kalman gain plays an important role in estimating the target's state, it is independent of the measurements taken. As can be seen from Fig 1 the right hand side frame is not affected by the observations, in fact, given the process and measurement noise covariances as a function of time, the Kalman gain can be computed off line.

During the recursive estimation of the state, the Kalman gain reaches a steady-state value determined by the pre-selected and assumed constant process and measurement noise covariances, Q and R respectively. The use of constant values of the covariances imposes a major restriction on the filter's performance, because if the pre-selected process noise covariance level is not appropriate the correction, by the Kalman gain, on the state prediction will not be suitable and large estimation errors will develop. An intiutive solution to this problem is to adaptively adjust the process noise covariance and thus the Kalman gain, according to changing target dynamics. The simplest method to achieve this is to establish a maneuver detection scheme then modify the process noise covariance following the maneuver detection [1]. The main disadvantage of this approach is the time delay in maneuver detection and changing of the filter. In [2] an adaptive Kalman filtering

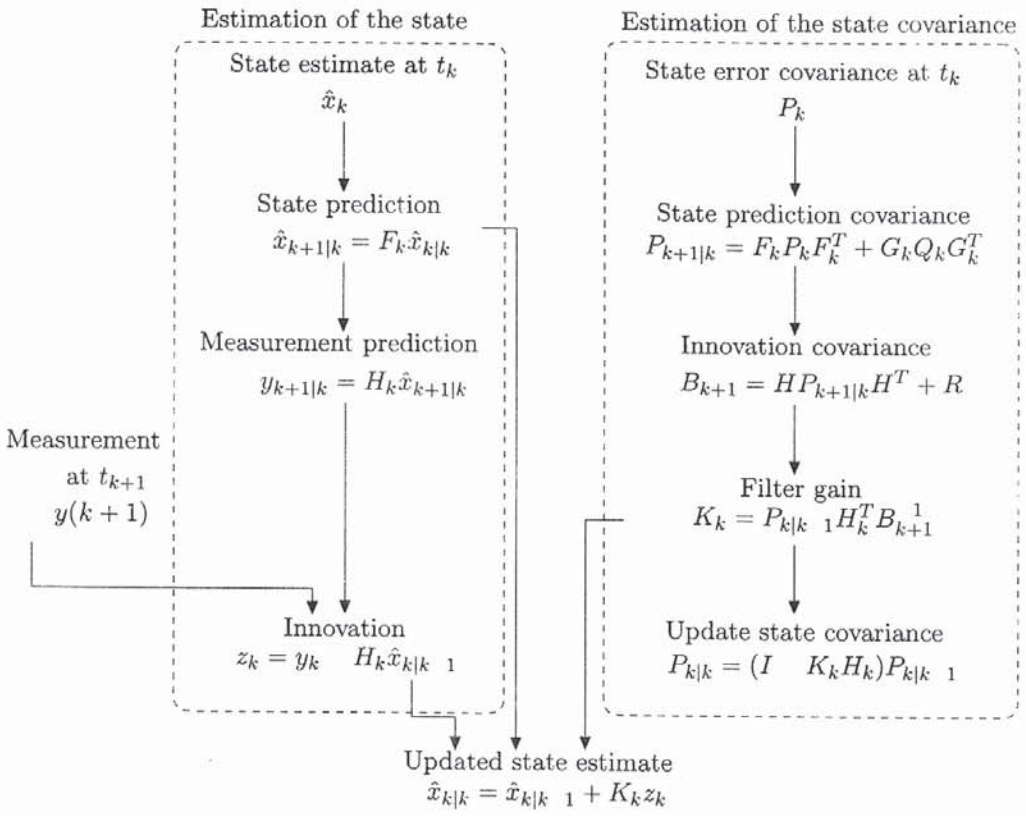

Figure 1: State Estimation Process in the Kalman Filter

technique was suggested where the process noise variance was estimated by means of the difference between the expected prediction error variance and the measurement noise variance. In [3] a new adaptive Kalman filter was suggested for tracking turn manoeuvres where the process noise covariance was associated with the turn rate through an empirical turn rate-process noise covariance curve. Alternatively, multiple model algorithms can be used, to provide good coverage with several levels of process noise covariance. The IMM algorithm is considered as one of the most efficient multiple model algorithms.The algorithm, which was introduced in [4], is derived from the multiple model approach, but unlike the multiple model structure, it keeps the number of hypotheses fixed, which reduces the computational burden. The algorithm employs a fixed number of models that interact through state mixing to track a maneuvering target. Every filter employed in the algorithm corresponds to a possible target motion to cover the actual modes of the target. The probability of each model being true is found by using a likelihood function for the model and switching between the models is governed by a transition probability

matrix. The state estimates from the subfilters are then mixed, by means of weighting coefficients, in order to get the combined state estimate. However, utilizing more models means increased computational burden and complexity and even a large number of models does not guarantee a better coverage. Although several adaptive methods [5], [6] have been suggested to limit the number of models used, a more complex structure and larger number of calculations result.

In this paper a novel method is presented to adjust the gain level of a second order Kalman filter for tracking manoeuvring targets. The method introduces a forgetting factor which represents the current magnitude of process noise covariance, in other words target unpredictability, at time n and is estimated from the available data. The aim of the proposed method is to take observations into account in the right hand frame of Fig 1, so that the Kalman gain level is adaptively adjusted in accordance with the changing target dynamics.

3 Fading Kalman Filter

Let us consider the following state-space model

$$x_{k+1} = F_k x_k + G_k w_k \tag{1}$$

$$y_k = H_k x_k + \nu_k \tag{2}$$

where x_k is the $n \times 1$ state vector, y_k is the $r \times 1$ observation vector, w_k is the $p \times 1$ state noise, ν_k is the $r \times 1$ observation noise at time k. F_k is the known $n \times n$ state transition matrix, G_k is the known $n \times p$ disturbance matrix and H_k is the $n \times r$ measurement matrix. Note that w_k and ν_k denote sequences of independent random vectors with zero means and covariance matrices Q_k and R_k respectively. The initial state x_0 is a random variable with zero mean and covariance matrix P_0 independent of w_k and ν_k.

Then the standard Kalman filter recursions are given as [7]

$$\hat{x}_{k+1|k} = F_k \hat{x}_{k|k} \tag{3}$$

$$P_{k+1|k} = F_k P_k F_k^T + G_k Q_k G_k^T \tag{4}$$

the time update and

$$\hat{x}_k = \hat{x}_{k|k-1} + K_k z_k \tag{5}$$

$$z_k = y_k - H_k \hat{x}_{k|k-1} \tag{6}$$

$$K_k = P_{k|k-1} H_k^T (H_k P_{k|k-1} H_k^T + R_k)^{-1} \tag{7}$$

$$P_k = (I - K_k H_k) P_{k|k-1} \tag{8}$$

the measurement update equations where K_k is the Kalman gain matrix and z_k is the residual vector. If the filter is constructed on the basis of an erroneous model, the error covariance matrix will become either too small, which will result in a small Kalman gain and subsequent observations will have a little effect on the estimate, or it will become too large and the filter will rely on the observations only. In [8] a new method was initiated to limit the memory of the Kalman filter by using exponential fading of past data through the use of a forgetting factor λ_k. The equations describing the fading Kalman filter are identical to those of the standard Kalman filter except for the forgetting factor inserted into the covariance equation which is given as

$$P_{k+1|k} = \lambda_{k+1} F_k P_k F_k^T + G_k Q_k G_k^T \tag{9}$$

with $\lambda_k \geq 1$. The performance of the exponetial fading Kalman filter fully depends on the selection of the forgetting factor. Therefore, the key problem is generating the optimal forgetting factor λ_k. The optimal way of calculating the forgetting factor λ_k was given in [9] and [10].

3.1 The Proposed Algorithm

Recursive least squares method has been used by many researchers to derive the Kalman filter. Let $\hat{x}_{k-1}$ be a priori estimate of x_{k-1} at time $k-1$ with covariance P_{k-1}. Then the time update equations are given as Eqs 3 and 4. Therefore $\hat{x}_{k|k-1}$ is a priori estimate of x_k with covariance $P_{k|k-1}$. Suppose we consider measurements y_k at time k and the prior information $\hat{x}_{k|k-1}$ described above, then

$$\hat{x}_{k|k-1} = x_k + e_k \tag{10}$$

$$y_k = H_k x_k + \nu_k \tag{11}$$

where e_k denote sequences of independent random vectors with zero mean and covariance matrix $P_{k|k-1}$. One way of combining the information in Eqs 10 and 11 is to minimize the following cost function

$$J_k = (x_k - \hat{x}_{k|k-1})^T P_{k|k-1}^{-1}(x_k - \hat{x}_{k|k-1}) + (y_k - H_k x_k)^T R_k^{-1}(y_k - H_k x_k) \tag{12}$$

The latter problem can be solved by differentiating this function and setting the derivative to zero and solve the resulting equations [11]. Another approach is to reduce the problem to the Gauss-Markov-Aitken theorem by expresing Eqs 10 and 11 as a single matrix equation [12]. This procedure results in

$$\begin{bmatrix} y_k \\ \hat{x}_{k|k-1} \end{bmatrix} = \begin{bmatrix} H_k \\ I \end{bmatrix} x_k + \begin{bmatrix} \nu_k \\ e_k \end{bmatrix} \tag{13}$$

Then applying the Gauss-Markov-Aitken theorem to the combined system, Eq 13, the best linear unbiased estimator $\hat{x}_k$ of x_k is

$$\hat{x}_k = P_k H_k R_k^{-1} y_k + P_k P_{k|k-1}^{-1} \hat{x}_{k|k-1} \tag{14}$$

and the corresponding covariance P_k is given by

$$P_k^{-1} = P_{k|k-1}^{-1} + H_k^T R_k^{-1} H_k \tag{15}$$

The matrix incersion lemma [7] is applied to Eq 15 in order to obtain the standard Kalman filter from Eq 14. This leads to the measurement update equations. From Eq 12 the prior expected value of J_k is

$$E[J_k] = trace(I_{n\times n}) + trace(I_{r\times r}) = n + r \tag{16}$$

In other words, if the Eq 16 holds, then the Kalman gain is optimal. If the filter is constructed on the basis of erroneous model estimate may diverge. Lets denote the actual value of J_k as $\hat{J}_k$ which should be computed by setting $x_k = \hat{x}_k$ after the estimation process has been completed at each scan. If $\hat{J}_k$ is not close to $n + r$ then the elements of $P_{k|k-1}$ and R_k must be multiplied by a scaling factor given as $\lambda_k^* = \hat{J}_k/(n + r)$ which adjusts the value of J_k to $n + r$. Note that this procedure also requires for P_k to be multiplied by the same scaling factor. Then the resulting error cavariance is given by

$$P_k^* = \lambda_k^* P_k \tag{17}$$

If $\hat{J}_k \leq E[J_k]$, then the filter is optimal (or capable) otherwise it may diverge. Also note that for $\lambda_k^* = 1$ the fading Kalman filter becomes the standard Kalman filter.

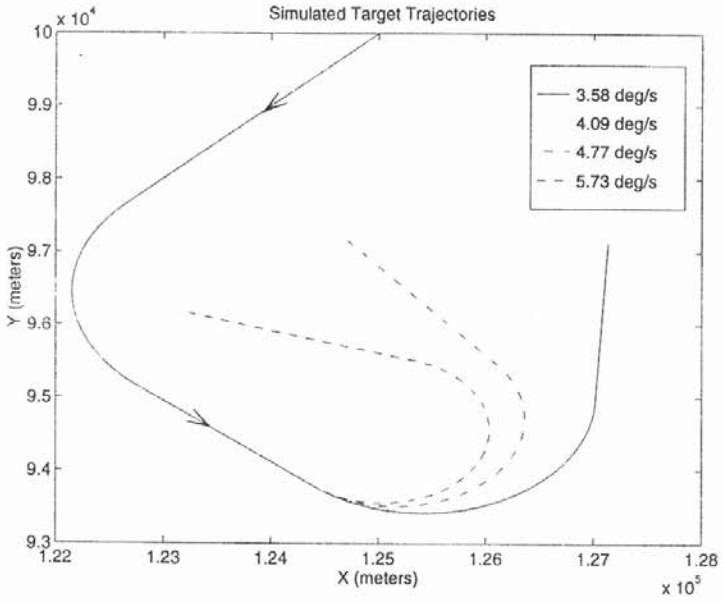

Figure 2: Simulated target trajectories

4 Simulation Results

The simulated target motion was generated in two dimensions (i.e. x-y plane) with a sampling interval of 1.0 second. Measurements were assumed known at the origin of the cartesian coordinates for the x-y positions of the target with a Gaussian measurement error standard deviation of 50 m used for both axes. Four target scenarios were chosen to perform a constant velocity motion with circular turns with initial velocities of 100 m/s in both axes, as depicted in Fig 2. The motion of each of the four targets is the same for the first 60 seconds and starts with 25 seconds of straight line motion, and then proceeds for a further 20 seconds turning with a 1.7 km. radius (3.37 deg/s turning rate) and there is another straight line path for 15 seconds. After that the targets exhibit a second turn, lasting 25 seconds with four different turning rates, where the turn rates are 3.58 deg/s for the first target, 4.09 deg/s for the second target, 4.77 deg/s for the third target and 5.73 deg/s for the fourth, they all conclude with 15 seconds of straight line motion.

The performance of the new filter is compared to those of an IMM algorithm and a second order Kalman filter utilizing fixed process noise modelling, which corresponds to $\lambda(k) = 1$ for all k in Eq 9. Two different assumptions were made for designing the IMM

algorithm and the second order Kalman filter. The first assumption, denoted '0', was that there was no prior information about the individual target motions and predetermined process noise covariance values were employed in the filters. The second assumption was that the largest turn rate that the target of interest would perform was known. Hence, a different set of process noise covariance levels was used for each target scenario, in both the IMM algorithm and the second order Kalman filter. The process noise covariance values employed in the IMM algorithm and the Kalman filter are given in Table 1.

Tracking Algorithm	Target1	Target2	Target3	Target4
	Process Noise Covariance $\times 10$ $((m/s^2)^2)$			
Ad. Kalm. filter	Fixed (with adaptively varying λ)			
IMM-0	1,7.5,15	1,7.5,15	1,7.5,15	1,7.5,15
IMM-1	1,6,12	1,8,16	1,10,20	1,12,24
Kalman-0	15	15	15	15
Kalman-1	12	16	20	24

Table 1: Process Noise Values employed in the filters

Three models were employed in the IMM-0 algorithm. The first model utilised a small process noise covariance value, namely 10 $(m/s^2)^2$, to model the straight line motion of the target. The second and the third models employed relatively larger process noise covariances to match the target motion during various manoeuvres. In the Kalman-0 algorithm a moderate level of process noise covariance was selected in order to both match the target motion during manoeuvres and provide moderate noise supression during nonmanoeuvring periods. For the second assumption, specific process noise covariance levels were chosen and utilized in both the IMM-1 and the Kalman-1 algorithms so that the filter kept on average the estimation errors slightly smaller than the measurements during the largest turn. Each of the five algorithms given in Table 1 was tested on the simulated scenarios. Performance of the algorithms was examined in terms of the normalized position error (NPE), which is the ratio of the root mean square of position

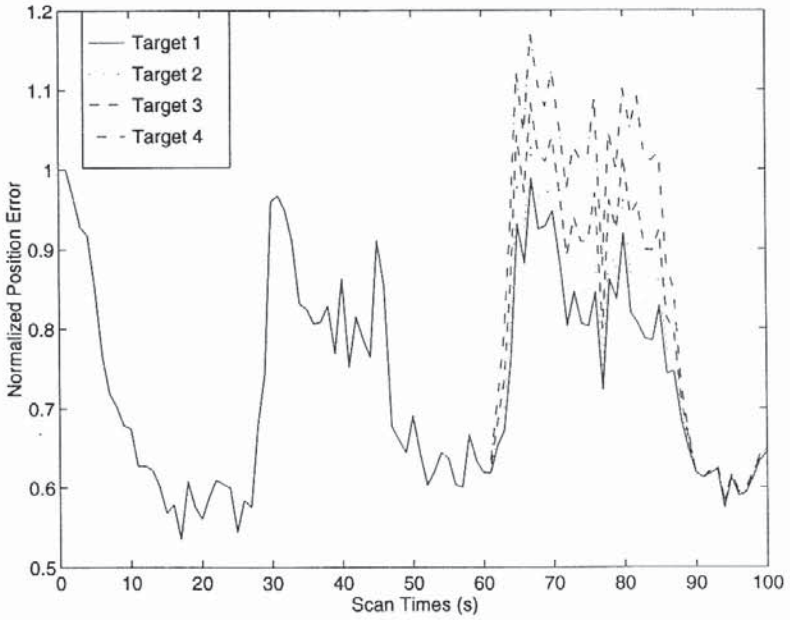

Figure 3: The NPEs of the IMM-0 algorithm for the scenarios

error to the root mean square of measurement error and given by

$$N.P.E.(k) = \frac{\sqrt{\frac{\sum_{i=1}^{N}[(x^i(k)-\hat{x}^i(k))^2+(y^i(k)-\hat{y}^i(k))^2]}{N}}}{\sqrt{\frac{\sum_{i=1}^{N}[(x^i(k)-z_x^i(k))^2+(y^i(k)-z_y^i(k))^2]}{N}}} \tag{18}$$

where $x^i(k)$, $y^i(k)$ and $\hat{x}^i(k)$, $\hat{y}^i(k)$ stand for the true and estimated positions of the target at the 'n'th scan in the 'i'th simulation run respectively. $z_x^i(k)$ and $z_y^i(k)$ are the measured x and y positions of the target and N is the total number of Monte Carlo runs. Figs 3 and 4 show the NPEs of the IMM-0 and Kalman-0 algorithms respectively for the scenarios where the predetermined process noise covariances were used in the filters for all the targets. During the second turn a clear performance degradation was observed for both the IMM-0 and Kalman-0 algorithms as the turning rate got larger. This is mainly because the steady state Kalman gain level yielded by the predetermined fixed process noise covariances employed in the filters was not high enough to cover the acceleration changes caused by larger turns. A higher Kalman gain level was needed to cover the larger turn manoeuvre, but since the process noise covariances were kept the same for all of the four targets, where the turn rate got larger, the steady state Kalman gain level remained the same. This is the major difficulty in manoeuvring target tracking with

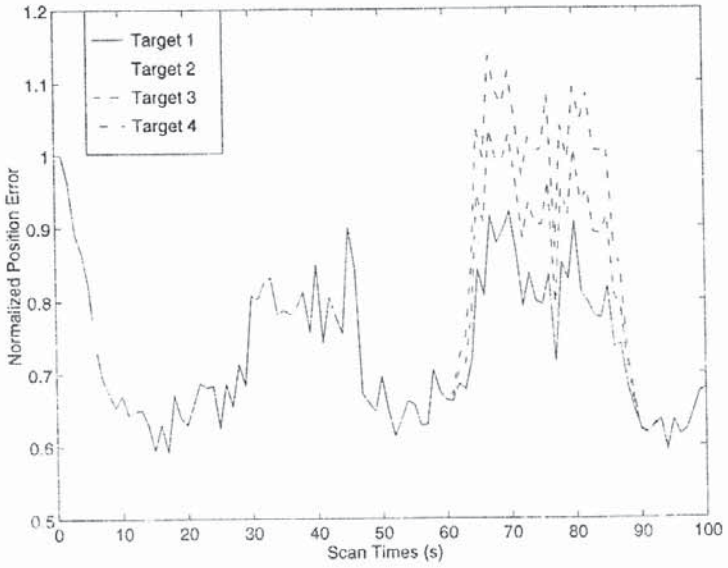

Figure 4: The NPEs of the Kalman-0 algorithm for the scenarios

fixed parameter modelling techniques. As soon as the target has initiated and sustained an unexpected manoeuvre, i.e., not covered by the predetermined modelling parameters, existing target models are no longer able to give good estimations.

But, as assumed in the second part of the experiments, if 'a priori' knowledge about the target motion is available, which is almost impossible in real life applications, an appropriate process noise covariance can be chosen to yield a better steady state Kalman gain. As can be seen from Fig 5 since the process noise covariance was chosen large enough to cover the biggest turn rate in each scenario, the IMM-1 algorithm kept its performance level almost the same for the different scenarios. On the other hand, a performance deterioration was observed during straight line motion and smaller turn periods due to the higher Kalman gain. The Kalman-1 algorithm also produced a very similar performance to the IMM-1 algorithm.

The adaptive Kalman filter, on the other hand, adaptively adjusted its Kalman gain level according to the changing target dynamics resulting in almost the same level of performance for different levels of turn rate. Fig 6 clearly shows that the position error for

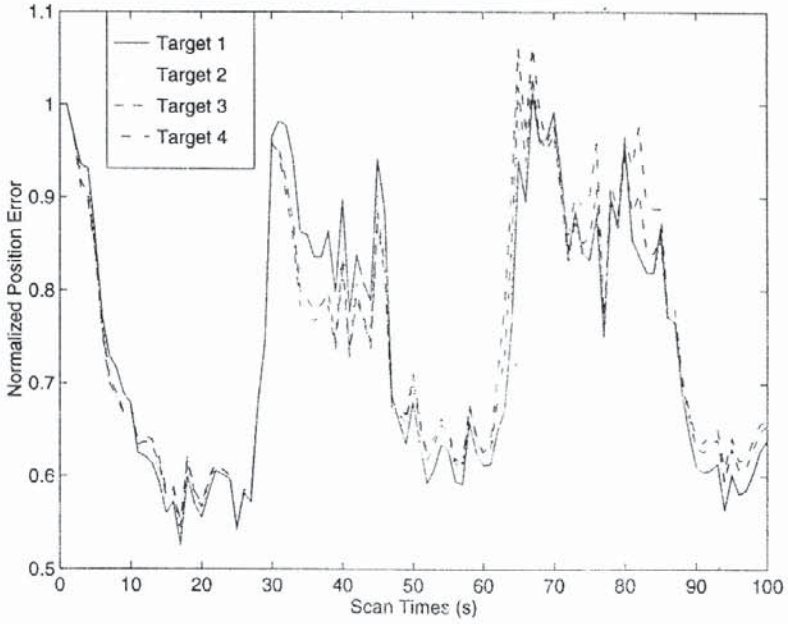

Figure 5: The NPEs of the IMM-1 algorithm for the scenarios

the adaptive filter remains almost the same whilst tracking larger turn rate manoeuvres. This was achieved by the use of the forgetting factor.

The fading Kalman filter has also been tested on another trajectory where the target exhibited a motion other than coordinated turns. In the scenario the target undergoes acceleration changes in both the x and y directions whilst going on a straight line path. The acceleration change is depicted in Fig 7. The performance of the fading Kalman filter is also shown in Fig 8. The filter, as expected, detects the acceleration change during both manoeuvring periods and adjusts its error covariance level to cover the changes without relying on a priori knwoledge of the target motions.

5 Conclusions

A novel adaptive Kalman filter has been presented. The Kalman gain level of the filter is adaptively adjusted at each time scan through the use of a scale factor which is calculated based on the available information. The scale factor level increases during manoeuvring

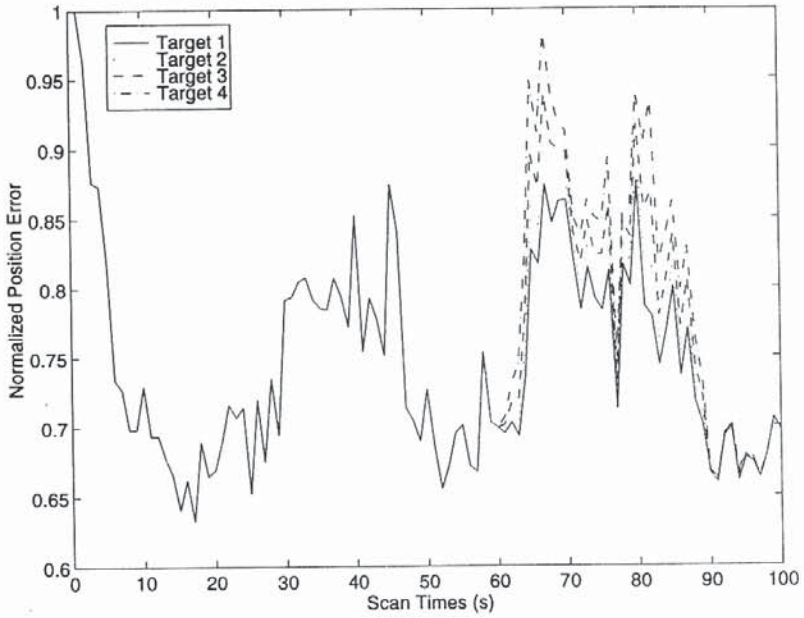

Figure 6: The NPEs of the fading Kalman filter for the scenarios

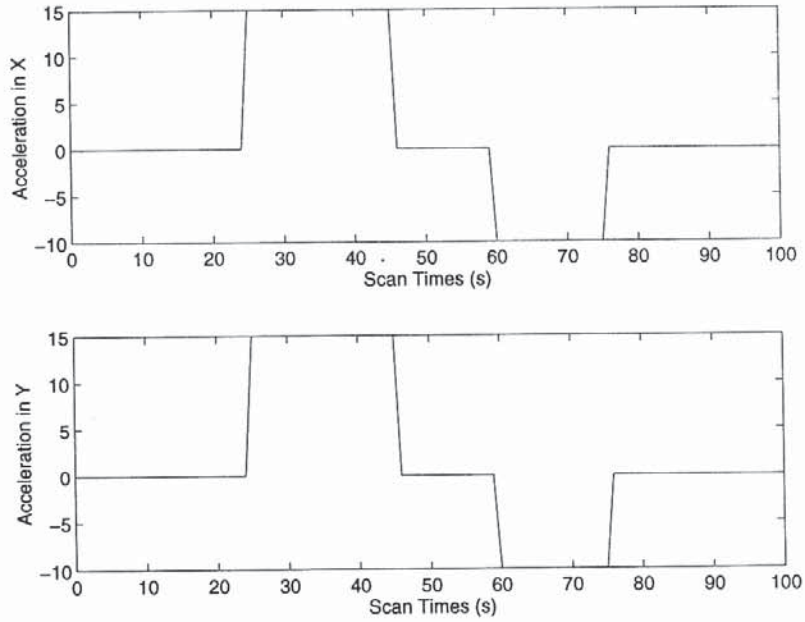

Figure 7: The acceleration change in the second scenario

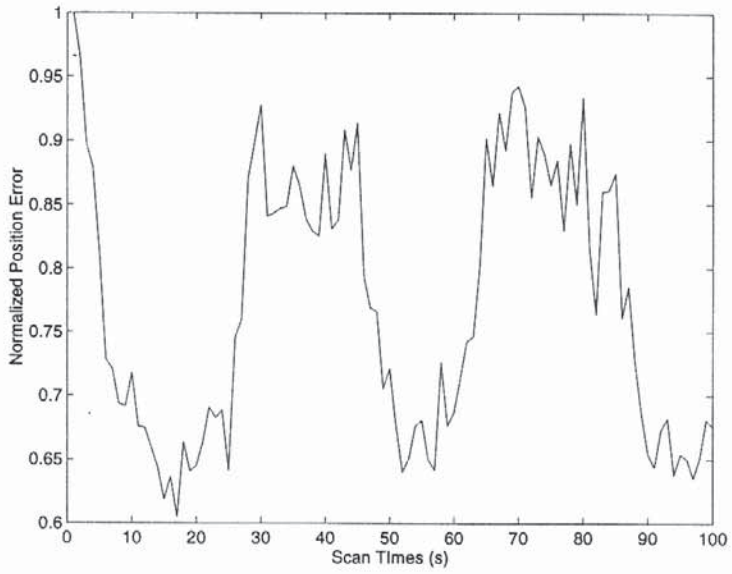

Figure 8: The performance of the fading Kalman filter on scenario 2

filter if some knowledge of the manoeuvre is assumed.

References

[1] Blackman, S.S., "Multiple-Target Tracking with Radar applications", Artech House, 1986

[2] Gutman, P.O., and Velger, M., "Tracking Targets Using Adaptive Kalman Filtering", IEEE Trans. on Aerospace and Electronic Systems, Vol-26, No. 5, September 1995, pp 691-698.

[3] Efe, M. and Atherton, D. P., "Maneuvering Target Tracking With an Adaptive Kalman Filter", 37th CDC Proceedings, December 1998, pp 737-742.

[4] Blom, H.A.P. "An Efficient Decision-Making-Free Filter For Processes With Abrupt Changes", IFAC Conference on Identification and System Parameter Estimation, 1985, pp 631-636.

[5] Li, X.R. and Bar-Shalom, Y., "Multiple Model Estimation with Variable Structure", IEEE Trans. on Automatic Control, Vol-41, No. 4, April 1996, pp 478-493.

[6] Efe, M. and Atherton, D. P., "Maneuvering Target Tracking Using Adaptive Turn Rate Models in The Interacting Multiple Model Algorithm", 35th CDC Proceedings, December 1996, pp 3151-3156.

[7] Jazwinski, A.H., "Stochastic Processes and Filtering Theory", Academic Press, 1970.

[8] Fagin, S.L., "Recursive Linear Regression Theory, Optimal Filter Theory and Error Analysis", Error Analysis IEEE Int. Conv. Rec., 12, 1964, pp 216-240.

[9] Xia, Q., Rao, M., Ying, Y. and Shen, X., "Adaptive Fading Kalman Filter With an Application", Automatica, Vol 30, 1994, pp 1333-1338.

[10] Ozbek, L. and Aliev, F.A., "Comments on Adaptive Fading Kalman Filter With an Application", Automatica, Vol 34, No 12, 1998, pp 1663-1664.

[11] Duncan, D.B. and Horn, S.D., "Linear Dynamic Recursive Estimation From the Viewpoint of Regression Anaylsis", JASA, 67. 1972, pp 815-821.

[12] Diderrich, G.R., "The Kalman Filter From the Perspective of Goldberger-Theil Estimators", The American Statistician, 39, No 3, 1985.

Özet

Bu makalede yeni bir adaptif Kalman filtreleme tekniği sunulmuştur. Sunulan filtre değişen hedef dinamiklerine göre durum hata kovaryansını ayarlayan bir unutma faktörü kullanmaktadır. Ayrıca filtre, elde bulunan bilgiyi kullanarak tum hedef hareketi suresince daha iyi bir takip sağlamayı amaçlamaktadır.